Research Paper

GEOSPHERE

GEOSPHERE, v. 17, no. 2

https://doi.org/10.1130/GES02267.1

19 figures; 1 supplemental file

CORRESPONDENCE: chrissmorley@gmail.com

CITATION: Morley, C.K., Jitmahantakul, S., von Hagke, C., Warren, J., and Linares, F., 2021, Development of an intra-carbonate detachment during thrusting: The variable influence of pressure solution on deformation style, Khao Khwang Fold and Thrust Belt, Thailand: Geosphere, v. 17, no. 2, p. 602–625, https://doi.org/10.1130/GES02267.1.

Science Editor: David E. Fastovsky
Associate Editor: Michael L. Williams

Received 4 April 2020
Revision received 31 August 2020
Accepted 29 October 2020

Published online 21 January 2021

Development of an intra-carbonate detachment during thrusting: The variable influence of pressure solution on deformation style, Khao Khwang Fold and Thrust Belt, Thailand

C.K. Morley[1], S. Jitmahantakul[2], C. von Hagke[3,4], J. Warren[5], and F. Linares[5]

[1]PTT Exploration and Production, Enco, Soi 11, Vibhavadi Rangsit Road, Chatuchak, Bangkok, 10900, Thailand
[2]Basin Analysis and Structural Evolution (BASE) Research Unit, Department of Geology, Faculty of Science, Chulalongkorn University, Bangkok, 10330, Thailand
[3]Institute of Geology & Palaeontology, RWTH Aachen University, Miner Building, Wullnerstrasse, 2, 52056, Aachen, Germany
[4]Department of Geography and Geology, Salzburg University, Hellbrunnerstraße 34, 5020 Salzburg, Austria
[5]Department of Geology, Faculty of Science, Chulalongkorn University, Phayathai Road, Bangkok, 10330, Thailand

ABSTRACT

Classic detachment zones in fold and thrust belts are generally defined by a weak lithology (typically salt or shale), often accompanied by high over-pressures. This study describes an atypical detachment that occurs entirely within a relatively strong Permian carbonate lithology, deformed during the Triassic Indosinian orogeny in Thailand under late diagenetic-anchimetamorphic conditions. The key differences between stratigraphic members that led to development of a detachment zone are bedding spacing and clay content. The lower, older, unit is the Khao Yai Member (KYM), which is a dark-gray to black, well-bedded, clay-rich limestone. The upper unit, the Na Phra Lan Member (NPM), comprises more massive, medium- to light-gray, commonly recrystallized limestones and marble. The KYM displays much tighter to even isoclinal, shorter-wavelength folds than the NPM. Pressure solution played a dominant role throughout the structural development—first forming early diagenetic bedding; later tectonic pressure solution preferentially followed this bedding instead of forming axial planar cleavage. The detachment zone between the two members is transitional over tens of meters. Moving up-section, tight to isoclinal folds with steeply inclined axial surfaces are replaced by folds with low-angle axial planes, thrusts, and thrust wedging, bed-parallel shearing, and by pressure solution along bedding-parallel seams (that reduce fold amplitude). In outcrops 100–300 m long, reduction of line-length shortening on folds from >50% to <10% shortening upwards indicates that deformation in the NPM is being accommodated differently from the KYM, probably predominantly by shortening on longer wavelength and/or spacing folds and thrusts, given the low amount of strain observed within the NPM, which excludes widespread layer-parallel thickening.

Christopher Morley https://orcid.org/0000-0002-6075-9022

INTRODUCTION

Lithological variations within fold and thrust belts can result in differences in deformation behavior and style of sedimentary layers separated by detachments, both at the base of, and within thrust sheets (Fig. 1; e.g., Dahlstrom, 1969; Geiser, 1988; Boyer and Mitra, 2019). Intra-thrust sheet detachments occur at a range of scales and enable separation of rock packages based on variations in one or a combination of the following inter-related characteristics: scale (e.g., fold wavelength and/or amplitude, fault spacing, and displacement magnitude) and style of structure (e.g., Dahlstrom, 1969; Morley, 1986, 1987; Wallace, 1993; Ghanadian et al., 2017); deformation mechanisms (e.g., brittle failure, diffusional flow, and intracrystalline plasticity; Davis and Engelder, 1985; Letouzey et al., 1995; Dean et al., 2013; Morgan, 2015; Meng and Hodgetts, 2019), and varying amounts of local strain (Morley, 1986, 1987; Boyer and Mitra, 2019).

At the largest scale, the basal detachment to a thrust belt separates overlying units deformed during a particular structural episode from underlying units undeformed by that episode, whereas higher-level detachments separate zones of different mechanical behavior within thrust sheets (Fig. 1). In well-described natural examples of detachments within sedimentary sequences, and in related analogue models, detachments are most widely associated with weak, commonly over-pressured lithologies, in particular, shales and evaporites, which can range from thick to thin zones and still be effective detachment horizons (e.g., Geiser, 1988; see reviews in Morley et al., 2011, 2017, 2018, and Ghanadian et al., 2017). However, detachment zones do not have to be confined to shales and evaporites, as discussed in this study; even relatively strong units, such as limestones, can develop detachment zones (Fig. 1D). Such intra-formational detachments are much less well understood than basal detachments. In this study, we describe the characteristics of a detachment zone within a thick sequence of Permian limestones, located in the Triassic Khao Khwang Fold and Thrust Belt (KKFTB) of Thailand (Fig. 2). This area is exceptional, because it offers spectacular outcrops of a detachment zone in typical passive margin carbonates. Of particular interest regarding this detachment is how variations in limestone clay content and spacing of bedding surfaces have influenced structural style in a carbonate platform sequence. The observations made in the KKFTB may serve as an example of how strain may be

localized in other orogens where passive margin carbonates are incorporated into a growing orogenic wedge, such as in the Oman Mountains or the European Alps.

GEOLOGICAL BACKGROUND

The KKFTB (Fig. 2B) developed between ca. 240–200 Ma, in multiple stages of deformation during the Triassic–Early Jurassic Indosinian orogeny (e.g., Morley et al., 2013; Arboit et al., 2016a; Hansberry et al., 2017). The Indosinian orogeny is related to subduction of the Paleo-Tethys ocean and the accretion of small continental fragments that formed the core of SE Asia (e.g., Metcalfe, 1999, 2011). Collision of the Sibumasu and Indochina continental terranes (Fig. 2B) marks the apex of the orogeny, following the closure of the Paleo-Tethys ocean (e.g., Sone and Metcalfe, 2008; Barber et al., 2011; Morley, 2018). The KKFTB lies within the Indochina Block (Fig. 2B) and is unusual because it trends approximately E-W, while the major Paleo-Tethys suture zone in Thailand trends N-S (Morley et al., 2013). The KKFTB is thought to mark a secondary suture zone between northern and southern crustal blocks that are both traditionally considered part of the Indochina Terrane (Morley et al., 2013). Structures verge mostly to the north, but areas of south-vergent structures locally occur, including the study area (Morley et al., 2013; Arboit et al., 2014; Hansberry et al., 2014). NW-SE– and NE-SW–oriented structures are present in some areas and either reflect superimposition of different non-coaxial structural events during the Indosinian orogeny, or inheritance of oblique features in the pre-collisional continental margin. Extensive quarrying for cement and marble has provided many well-exposed examples of fold and thrust structures, within Permian platform carbonates (e.g., Morley et al., 2013; Arboit et al., 2014, 2016a; Hansberry et al., 2014; Morley et al., 2017), while within the deeper-water shale, chert, and calci-turbidite units, there are numerous quarries for road aggregate and slate. The temperature during deformation of the KKFTB has been estimated from illite crystallinity values from Permian shales to the upper diagenetic zone to lowermost metamorphic zone (~160–220 °C; Hansberry et al., 2015). These values are consistent with the occurrence of pencil to slaty cleavage. Thin sections from the study area show calcite twins range between Type I (thin twins), Type II (tabular thick twins), as well as Type III (bent twins) following the nomenclature of Burkhard (1993). This indicates lower anchizonal temperatures (<250 °C; Burkhard, 1993; Ferrill et al., 2004).

There is also an extensive history of arc-type intrusive activity from the Late Permian to the Late Triassic (Arboit et al., 2016b). The intrusions (typically dikes and sills) tend to be andesitic in composition, with some dacitic-rhyolitic intrusions occurring (Arboit et al., 2016b). Dikes and sills can be up to several meters thick. These intrusions range from Late Permian to Late Triassic in age; rhyolitic dikes are mostly Late Triassic (Arboit et al., 2016b). While the majority of dikes and sills appear to postdate deformation, some are folded.

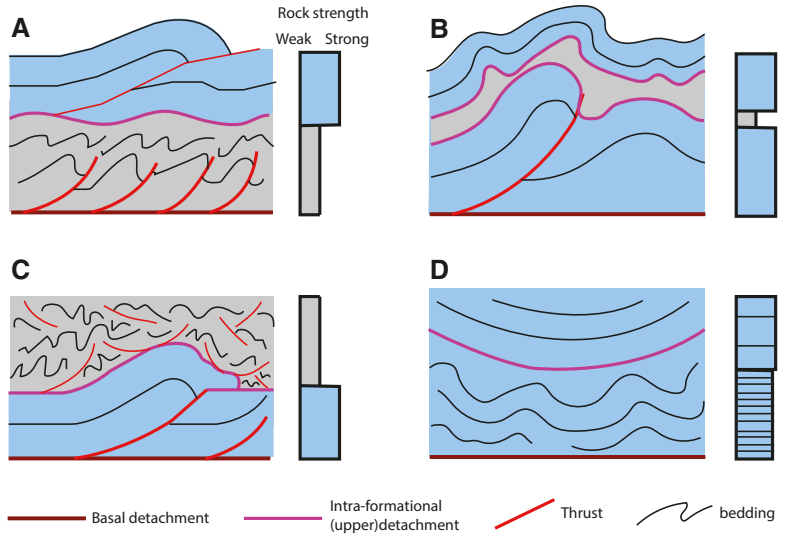

Figure 1. Schematic cross sections illustrating some basic intra-thrust sheet detachment behavior based on mechanical stratigraphy. (A) Relatively weak unit overlain by strong unit; (B) a narrow weak unit acts as a detachment zone between two stronger units; (C) relatively weak unit overlies strong unit; (D) strong units, but with more closely spaced bedding in the lower unit causing shorter wavelength folding than in the upper unit.

Stratigraphy

An early stratigraphic scheme for western Indochina Terrane Permian deposits in Thailand identified two carbonate platforms (Khao Khwang and Pha Nok Khao), separated by a deep-water basin represented by the Permian Nam Duk Formation (Fig. 2B; Wielchowsky and Young, 1985). The age of this platform sequence ranges from Asselian to Midian (Capitanian) (e.g., Toriyama, 1975; Altermann et al., 1983; Chonglakmani and Fontaine, 1992), and together these units comprise the Saraburi Group (Bunopas, 1981; Kozar et al., 1992; Chantong, 2005). Seismic-reflection data and drilling in the Khorat Plateau area have revealed that the Pha Nok Khao Formation comprises small carbonate platforms located on structural highs in a rift setting, separated by deeper-water clastic rocks deposited in extensional basins between the highs (Booth and Sattayarak, 2011). The Khao Khwang

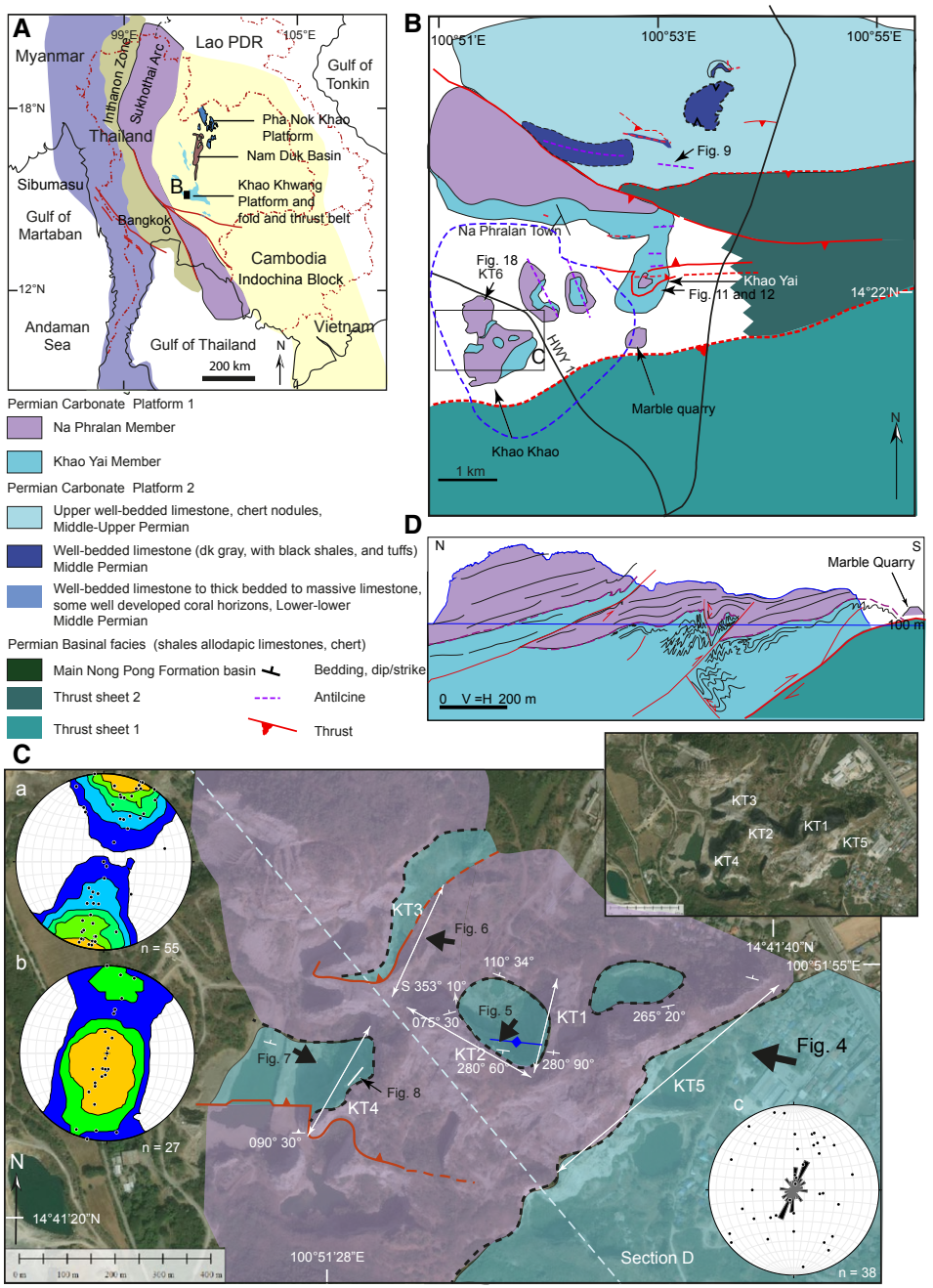

Figure 2. (A) Regional location map of SE Asia, showing main tectonic zones of the Indosinian orogeny (continental terranes—Sibumasu, Indochina; Paleotethys suture—Inthanon Zone; island arc sequence—Sukhothai Arc). Permian carbonate platforms—Pha Nok Khao Platform, Khao Khwang Platform. (B) Geological map of the Na Phra Lan area (see A for location). (C) Geological map of the study area (Khao Khao) adjacent to Na Phra Lan Town (see B for location), a—poles to bedding for the Khao Yai Member, b—poles to bedding for the Na Phra Lan Member, c—calcite slickenside orientations (mostly related to bedding plane slip), the striations show a predominant NNE-SSW direction, but also a wide variety of orientations due to blocks being squeezed in a variety of directions as folds tightened up. (D) Cross section through the hilly region (Khao Khao) of the study area. See (C) for location.

Platform (Dew et al., 2018) is only known through surface outcrops. Like the Pha Nok Khao Formation (Booth and Sattayarak, 2011), the initial depositional environment for the Khao Khwang Platform was a number of small carbonate platforms separated by deep-water troughs filled by cherts, shales, and allodapic limestones (Fig. 2A; Hinthong, 1981; Hinthong et al., 1985; Ueno and Charoentitirat, 2011 Morley et al., 2013; Arboit et al., 2014; Warren et al., 2014; Dew et al., 2018; Vattanasak et al., 2020). The stratigraphy and sedimentology of the Khao Khwang Platform carbonates have been addressed in a number of studies (Dawson and Racey, 1993; Chonglakmani, 2001; Udchachon et al., 2007; Dew et al., 2018), with the latest revisions to the stratigraphy reviewed in Dew et al. (2018).

The shelfal Permian limestones and marbles exposed in the study area around the town of Na Phra Lan are part of the late Early Permian to early Late Permian, Khao Khad Formation (Ueno and Charoentitirat, 2011; Dew et al., 2018), where two members can be mapped out (Figs. 2 and 3). The lower member comprises dark-gray to black, well-bedded limestones, and occasional dolomitic limestones, with bedding surfaces spaced between ~10 cm to several meters apart. Lithofacies include bioclastic packstones, bioclastic wackestones, calcisphere wackestones, mudstones, and aggregated grainstones. All lithofacies contain high proportions of mud or numerous micritic grains. In places, thin (1–10-cm-thick) black shales are interbedded

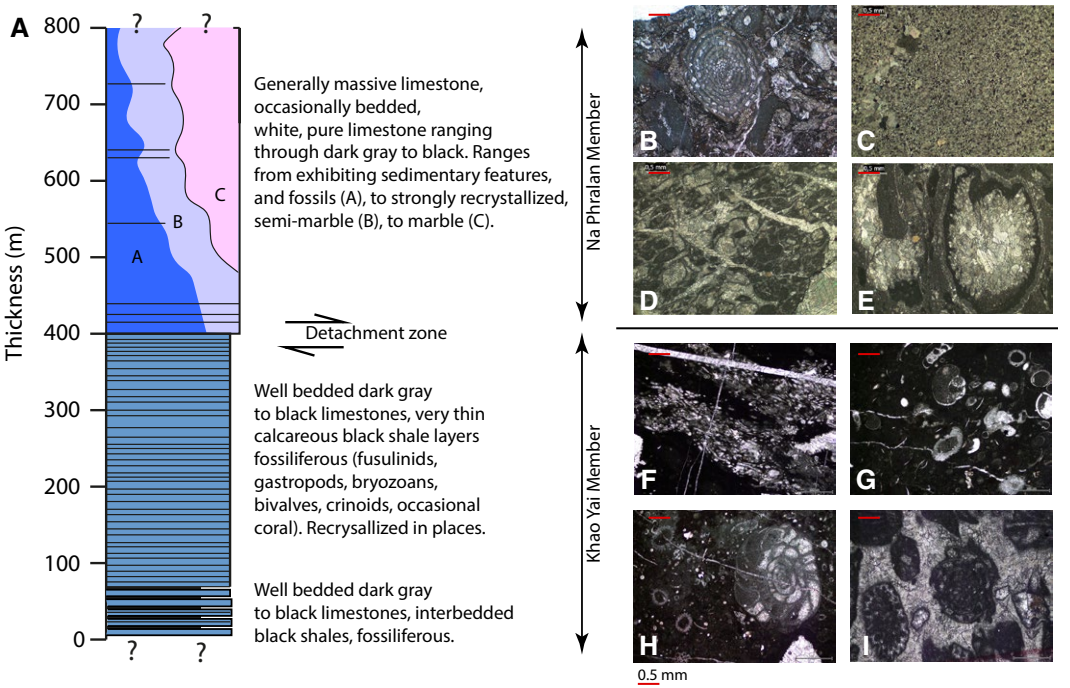

Figure 3. (A) Schematic stratigraphic section for the Middle–early Late Permian platform carbonates of the Khao Khad Formation in the Na Phra Lan area. Locally, the formation is divided into the lower, well-bedded, Khao Yai Member, and the upper more massive Na Phra Lan Member (see Fig. 3 for location of the study area). (B–E) Thin sections from the Na Phra Lan Formation; (B) bioclastic packstone, with prominent fusulinid; (C) fine-grained marble; (D) pelloidal and bioclastic packstone, with several generations of veins; (E) wackestone, with early cement infilling the cavity of a bivalve shell; (F–I) thin sections from relatively lightly deformed Khao Yai Formation, from the Khao Yai Hill area; (F) recrystallized coral in black micritic limestone; (G) wackestone, with bivalve and gastropod fragments; (H) wackestone with fossil including large fusulinid; (I) fusulinids surrounded by early sparry marine cement.

with the limestones. The limestones are sometimes strongly recrystallized but also commonly display sedimentary features and are fossiliferous, including: gastropods, bivalves, foraminifera (particularly fusulinids), bryozoans, framework-building algae, crinoids, and much less frequently corals and ammonoids. This sequence is well exposed in multiple quarries around a hill called Khao Yai (Fig. 2B); hence, the well-bedded limestones are referred to here as the Khao Yai Member.

Stratigraphically overlying the Khao Yai Member is the Na Phra Lan Member (Fig. 3). Both units are >400 m thick. In contrast to the well-bedded Khao Yai Member, the Na Phra Lan Member is a more massive unit. The Na Phra Lan Member generally displays widely spaced bedding surfaces >10–20 m apart, although locally several (two to six) closely spaced bedding surfaces can occur in intervals <10 m thick. The degree of recrystallization in the Na Phra Lan Member is highly variable; in the southern part of the area, the Na Phra Lan Member is quarried as a white marble for interior decoration. However, 4 km to the north, the member is quarried as a medium-gray, bioclastic grainstone, with a low degree of recrystallization. In the study area, the Na Phra Lan Member ranges between being strongly recrystallized, light-gray limestone with no fossils, to partially recrystallized bioclastic wackestones, grainstones, and packstones with corals, bryozoans, bivalves, and fusulinids still visible (Fig. 3). In some places, the limestone is medium gray to black in color, including a black marble that is quarried in the study area.

Burial and Exhumation History

Over the past ten years, we have built a substantial database on the O and C stable isotope signatures of vein material from the Saraburi Group in numerous Master of Science projects (see Warren et al., 2014, for a summary of the early results). The results of analyzing the stable oxygen and carbon isotope signatures of more than 1000 veins from the Saraburi Group show a broad range of burial history. Some less deformed outcrops provide a record of early marine cements in primary pores and vugs (Supplemental Data[1], Fig. S14E). Calcite bedding-plane slip regions provide many samples that plot in the negative carbon-isotope field since they are associated with thin layers of organic-rich shale that probably matured by burial during thrusting, and hence there is a catagenic influence. A widespread trend is that the earlier veins display relatively small negative $\delta^{18}O_{pdb}$ (Pee Dee belemnite) values, while major thrusts and later veins tend to display larger negative $\delta^{18}O_{pdb}$ values (Warren et al., 2014). In part, the trends reflect the loss of matrix permeability accompanying burial, with burial occurring both during deposition and

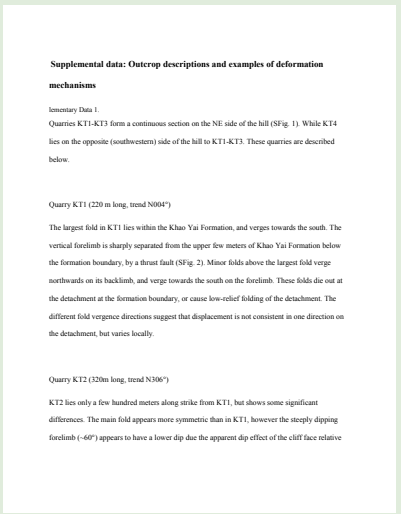

Supplemental data: Outcrop descriptions and examples of deformation mechanisms

lementary Data 1

Quarries KT1-KT3 form a continuous section on the NE side of the hill (SFig. 1). While KT4 lies on the opposite (southwestern) side of the hill to KT1-KT3. These quarries are described below.

Quarry KT1 (220 m long, trend N004°)

The largest fold in KT1 lies within the Khao Yai Formation, and verges towards the south. The vertical forelimb is sharply separated from the upper few meters of Khao Yai Formation below the formation boundary, by a thrust fault (SFig. 2). Minor folds above the largest fold verge northwards on its backlimb, and verge towards the south on the forelimb. These folds die out at the detachment at the formation boundary, or cause low-relief folding of the detachment. The different fold vergence directions suggest that displacement is not consistent in one direction on the detachment, but varies locally.

Quarry KT2 (320m long, trend N306°)

KT2 lies only a few hundred meters along strike from KT1, but shows some significant differences. The main fold appears more symmetric than in KT1, however the steeply dipping forelimb (~60°) appears to have a lower dip due the apparent dip effect of the cliff face relative

[1]Supplemental Data. Additional descriptions of outcrop data, thin sections, and limestone composition. Please visit https://doi.org/10.1130/GEOS.S.13166741 to access the supplemental material, and contact editing@geosociety.org with any questions.

deformation. The larger negative $\delta^{18}O_{pdb}$ values along some thrusts compared to the values in the host rocks indicate tapping of deeper, hotter fluids than just those from the formation (Warren et al., 2014). The stable isotope results from the NPM and the KYM are very similar and conform with the general trends observed in the region described by Warren et al. (2014). There is no apparent difference in the characteristics of veins and host-rock samples from the marble and from the KYM, with no significant difference in temperature to indicate contact metamorphism of the marble, raising the question of whether recrystallization could form marble at least partly related to deformation. Host and vein samples found around folds typically exhibit similar values indicating derivation of the veins from the host rock, most probably by pressure-solution processes. Hence, vein intensity around folds is a good indication of the intensity of pressure-solution activity.

Initial results on U-Pb dating of some veins within the Saraburi Group indicate that there is commonly a complex multiphase history to some veins (particularly along thrusts); this history makes dating unreliable, with large error bars. However, some of the smaller, simpler veins (i.e., those associated with flexural slip and small veins at a high angle to bedding developed during folding) can be dated and have yielded Late Triassic ages (A.D. Simpson, personal commun., 2020).

METHODOLOGY

The study area is part of a remapping project of the Khao Khwang Fold and Thrust Belt, which has been ongoing since 2011. Investigation into the KKFTB has been the subject of two Bachelor of Science honors projects, nine Master of Science projects, and two Ph.D. thesis projects from Chulalongkorn and Adelaide universities. Of these studies, a Bachelor of Science project (Dew et al., 2018), two Master of Science projects (Morley et al., 2013), and a Ph.D. project (Arboit et al., 2014, 2016a, 2016b, 2017) have conducted work that impacts the study area, including: (1) Establishing ages of the formations both from previous work and dating of new samples, which is primarily based on the dating of fusulinids (e.g., Ueno and Charoentitirat, 2011; Dew et al., 2018). (2) Recording of basic structural orientation data on bedding, folds, cleavage and faults (Morley et al., 2013; Arboit et al., 2014). (3) Description of host rock and vein textures in outcrop and thin section, which shows that veins related to folding and thrusting are commonly arrayed in patterns such as high angle to bedding, parallel to bedding (flexural slip), parallel to thrusts, en echelon tension gashes, and parallel to high-angle faults (Warren et al., 2014). The vein patterns show variability with structural position, where major thrusts and the tight cores of folds tend to show the greatest complexity of vein density, orientation, and types (Warren et al., 2014; Morley et al., 2017; see Supplemental Data [footnote 1]). (4) Sampling calcite veins for stable oxygen and carbon isotopes in order to determine fluid origin, relative temperatures of different vein sets, and host-rock porosity and permeability development (Warren et al., 2014). (5) Analyzing the calcite veins to determine paleo-stress (Arboit et al., 2017). (6) A pilot study to determine the feasibility of U-Pb dating of calcite veins (A.D. Simpson, personal commun., 2020). (7) Mapping of structures and lithological units, making descriptions and sections of the quarry faces (Morley et al., 2017). (8) Use of drones to record some quarry faces and to map the entire hill of Khao Yai. Some of this work is utilized in this study, together with new fieldwork and gathering of drone images to add extra structural detail regarding the nature of the detachment zone. Essential to the descriptions of the variations in deformation style across the detachment between the Khao Yai and Na Phra Lan members are photographs and sketches of structures of deformed limestones in the field; these sketches require tracing of bedding surfaces. The origin of bedding in limestones can be problematic, because while some bedding is primary depositional bedding, other bedding can form during compaction by pressure dissolution, with fissile limestones favoring development of bedding (dissolution seams, not stylolites), and hard limestones showing much less development of diagenetic bedding (Bathurst, 1987).

RESULTS

The area around the town of Na Phra Lan is composed of hills of Permian Khao Khad Formation limestones, which, to varying degrees, have been quarried. The Khao Khad Formation stratigraphically underlies the Na Phra Lan Formation and is exposed in cores of anticlines and culminations (Fig. 2). Permian folds and thrusts predominantly trend E-W to NW-SE in the study area. The key focus of this study is the Khao Khao area (Fig. 2C), which comprises a small range of hills (1.7 km NW-SE, 1.4 km NE-SW) that rise up to 160 m above the elevation of the town (~100 m above sea level) and lie on the west side of Highway 1. The detachment zone between the Khao Yai and Na Phra Lan Members is best exposed in the quarries around Khao Khao; hence, this area is the focus of this study. However, adjacent hills (in particular, Khao Yai and the marble quarry, Fig. 2B) also provide important information on the structural styles of the two members.

Structural Styles at Khao Khao

Khao Khao is extensively quarried on all sides (Fig. 2C), which is vital for revealing the structure of the hill. Overall, the Na Phra Lan Member gently dips ~8°–16° NNE, although in some places, it is folded and thrusted (Figs. 2C and 2D). The underlying Khao Yai Member is seen in four places (Fig. 2C): (1) a strike-oblique section on the south side of the hill (Fig. 4); (2) a culmination on the NE side of the hill (Fig. 5 and Supplemental Data [footnote 1]); (3) a thrust zone on the NE side of the hill (Fig. 6); and (4) the continuation of the culmination on the SW side of the hill (Figs. 7 and 8). Generally, a similar structural style is seen in all the outcrops, where tight folds and thrusts affect the Khao Yai, while the contact with the Na Phra Lan Member is straight to very gently warped (Fig. 4). Two areas reveal the same overall culmination on the NE and SW sides of the hill (Fig. 2C) and show contrasts between the strongly folded Khao Yai Member and the general low dips and gentle folding of the Na Phra Lan Member (Figs. 2C and 2D). Brief descriptions of

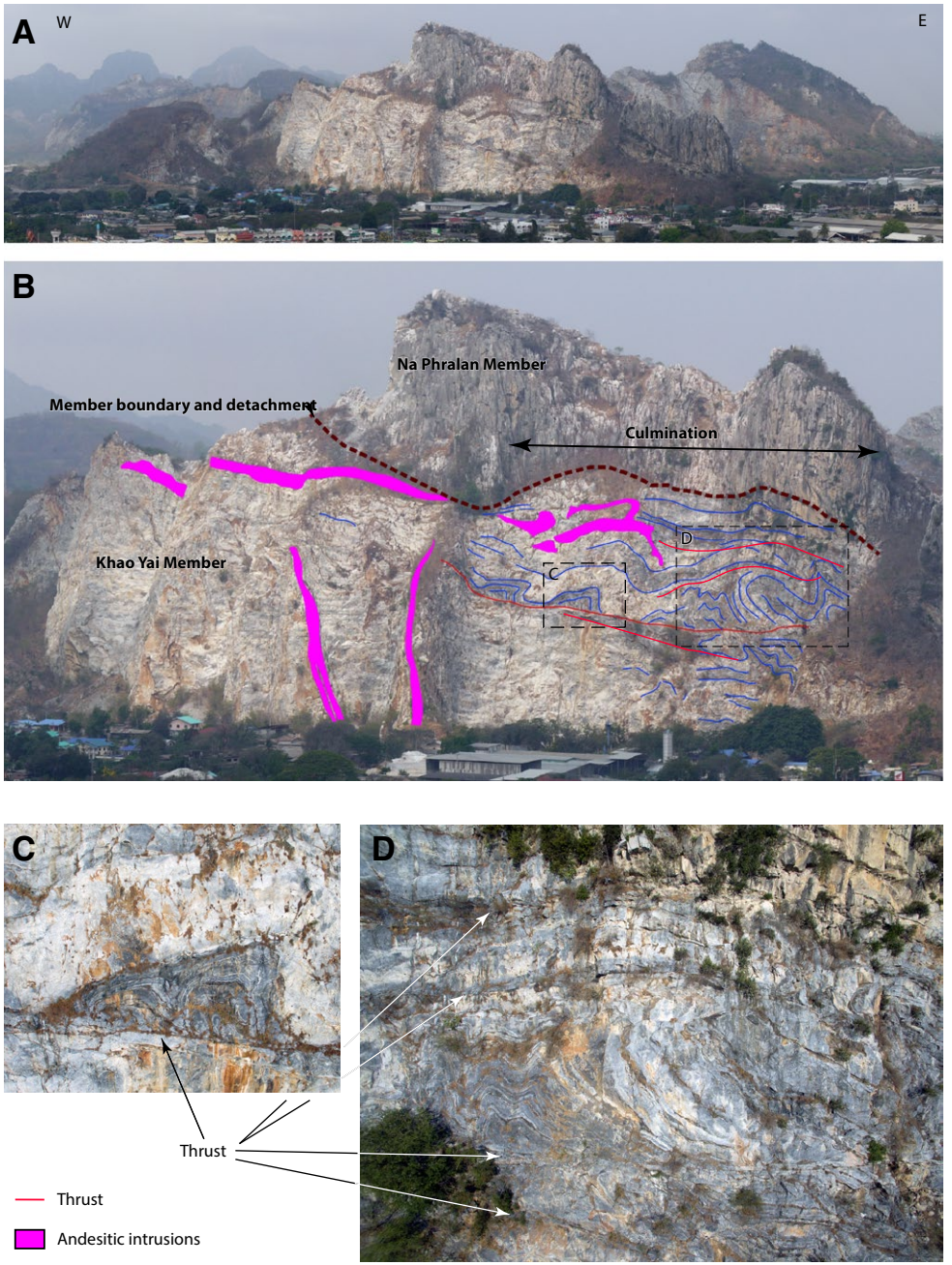

Figure 4. View to the north of Khao Khao, showing quarry KT5 (see Figs. 2B and 2C for location). (A) Overview of the quarried hill adjacent to the town of Na Phra Lan, view from the marble quarry in Na Phra Lan. (B) Detail of (A) showing the massive carbonate of the Na Phra Lan Member overlying the well-bedded Khao Yai Member. A number of Late Permian–Late Triassic andesitic intrusions are also present. On the eastern half of the cliff face the Khao Yai member is strongly deformed by folds and thrusts, in contrast the contact between the two members is not affected by intense folding, and is inferred to be acting as a detachment separating two different deformation styles. (C) Detail of folding above a thrust. (D) Detail showing folding and thrusting within the Khao Yai Member. The view is highly oblique to the tectonic transport direction.

the Khao Khao quarries are provided in the Supplemental Data (Figs. S1–S10, S12–S17).

Khao Yai Member

There are a few locations where the limestones are deformed by large, broad faults, but at the outcrop scale, deformation is low intensity and so provides a good starting point for understanding the state of the KYM prior to deformation (see Supplemental Data, Fig. S4). The KYM limestones are typically dark-gray to black, but weathering of some layers causes them to form a thin (<1 mm), light-gray buff surface layer that gives the appearance of alternating dark- and light-colored beds. Some limestone layers are more argillaceous than others, and in some parts of the stratigraphy, black shales are interbedded with limestones. Weakly deformed areas of the KYM are characterized by alternating stratigraphic layers that in general show only minor modification of bedding by pressure solution. Only a few scattered calcite veins at a high angle to bedding and along bedding surfaces are present.

One tight, asymmetric fold offers a rare opportunity to see the magnitude and consistency of flexural slip, because in the forelimb of the fold, three pre-kinematic andesitic dikes are offset by bedding plane slip (Fig. 9). In the example, flexural slip occurred on bedding surfaces spaced ~40 cm to 2 m apart, with offset of the dike segments in the order of 10 cm–1 m at each bedding surface.

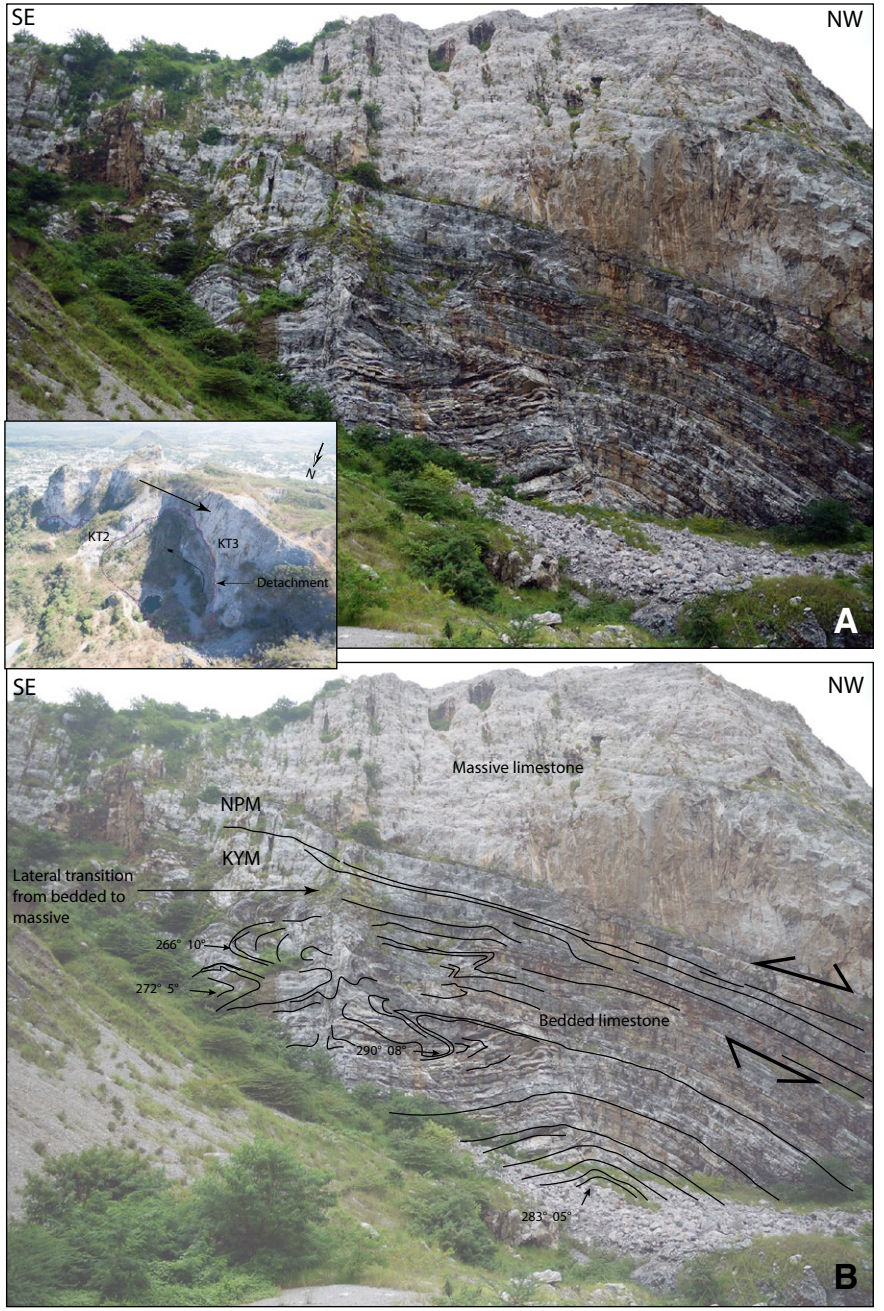

Figure 5. View to the SW of the quarry KT2. See Fig. 2C for location. (A) Uninterpreted photo; (B) interpreted photo. The detachment between the Na Phra Lan and Khao Yai members is a planar feature, whereas the Khao Yai Member is strongly folded. Within 10–20 m vertical distance below, the detachment folds with gently inclined to subhorizontal axial surfaces are present that verge both toward the south and the north. This quarry face also shows the issue of lateral changes near the base of the Na Phra Lan Member from massive to more regularly bedded units.

The sense of offset (right lateral, toward the fold axis) is typical of classic flexural slip models (e.g., de Sitter, 1958; Ramsay, 1974). These bedding surfaces, which offset dikes, show bed-parallel striated calcite veins, with striations that plunge in the dip direction. However, most of these surfaces could no longer undergo flexural slip because they have been affected by later pressure solution, which to greater or lesser degrees has irregularly crenulated the bedding surface (see Fig. 9, location X, for a strongly crenulated example). Some bedding surfaces have not undergone flexural slip because they do not offset the dikes—these are comparatively rare. Of the 26 modified bedding surfaces that intersect the dikes, 20 are offset dikes. The other six surfaces are bedding that has been modified by syn-tectonic pressure solution. Figure 9 is a relatively simple example of a fold, but what is apparent in this example is that there are virtually no original bedding surfaces remaining. Bedding has been modified by flexural slip and by pressure solution. Additionally, in the KKFTB, wedge thrusts (cf. Cloos, 1964 and Mitra, 2002) are common features in thick limestones beds, where deformation cannot be accommodated by flexural slip. Typically, such wedge thrusts in the KKFTB have tens of centimeters to a few meters displacement. Because of these three pervasive processes, the term modified bedding surface (MBS) is used here. Most commonly, significant development of MBS stylolites has developed along MBSs after flexural slip. There are a few places where the MBSs disappear laterally, despite showing offset on dikes just 2–3 m away (Fig. 9, location X). Eradication of the MBS trace occurs due to later deformation involving veining, recrystallization, and tectonic stylolites (e.g., Fig. 9,

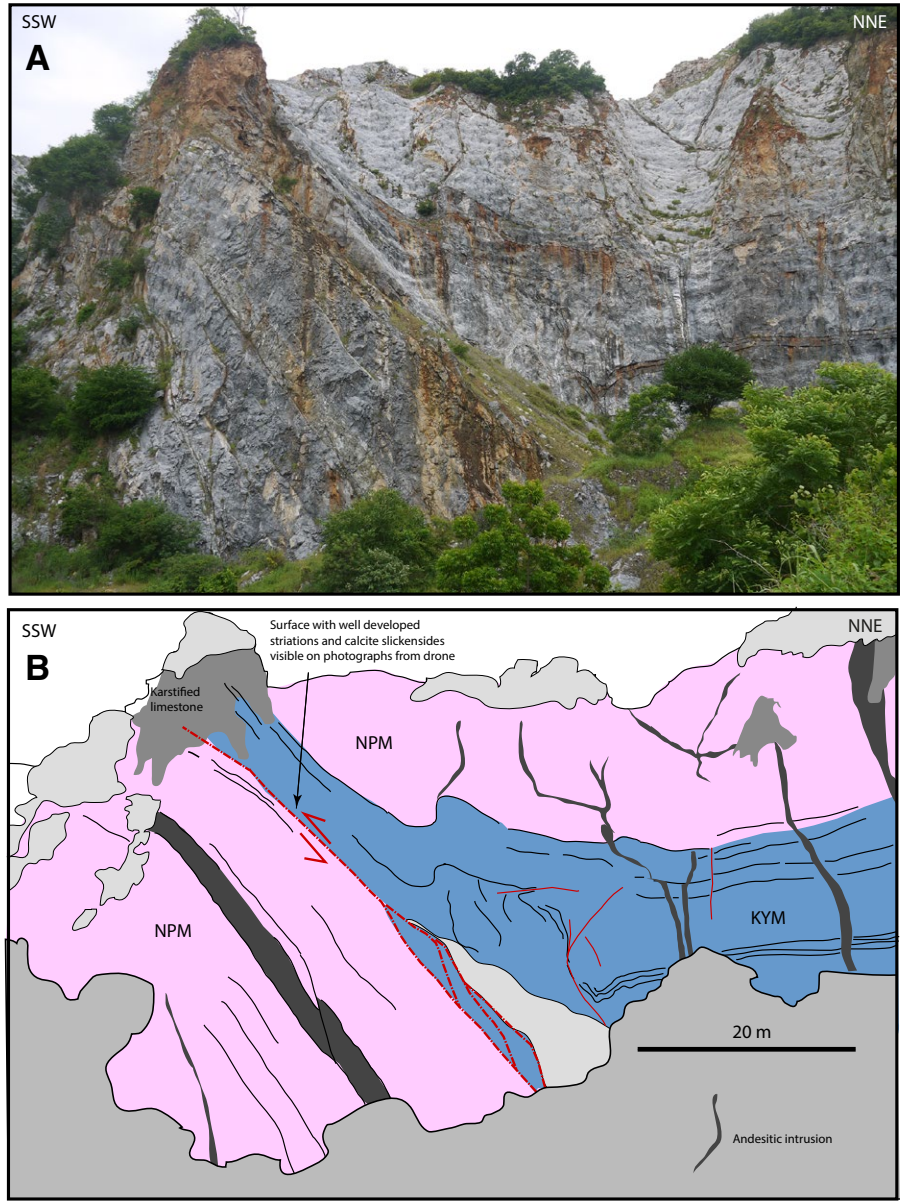

Figure 6. View to the W of the quarry KT3, which is structurally continuous with KT2. See Figure 2C for location. (A) Uninterpreted photo; (B) interpreted photo. A well-bedded unit (here interpreted as the Khao Yai Member) is thrust over massive Na Phra Lan Member carbonates that are intruded by a sill that itself is affected by a minor thrust. Bedding in the Khao Yai Member is not as clearly developed as in Figure 5.

location Y). Alternatively, some pressure-solution seams form shale-rich layers up to several centimeters thick as a consequence of concentration of insoluable material. Such layers are zones of weakness within a carbonate zone, and they tend to be sites of late slip, as indicated by the presence of polished, striated, graphitic shale surfaces accompanied by wavy, anastomosing shale fabrics and calcite slickensides. Examples and further descriptions of pressure solution and vein development are provided in the Supplemental Data and Figures S5–S9, S12, S13, and S16 (footnote 1).

The KYM is typically dark gray to black in color, while packstones and grainstones are present in the KYM. Most commonly, it is composed of calcareous mudstones and wackestones. While a black limestone may simply indicate its fine-grained nature and have nothing to do with clay content, for the KYM, in many places, thin shales are interbedded with the limestones, indicating clay content is a likely factor. The clay content is also indicated by the presence of clay selvages along pressure-solution seams, which in extreme cases can be 1–2 cm thick.

For three typical KYM samples, Al_2O_3 ranged between 0.12 wt% and 1.12 wt%, while in two limestones with well-developed, thick pressure-solution seams, the Al_2O_3 content was 3.46 wt% and 7.22 wt%. Silica content was also high (5.66 wt% and 12.47 wt%) in these two samples compared with <0.63 wt% in five other samples and 2.18 wt% in one from both the KYM and NPM. Hence, clay content is highly variable within the KYM, but for some beds is distinctly higher than in the NPM.

The two highest Al_2O_3 content samples (KYM) contain pyrophyllite ($Al_2Si_4O_{10}(OH)_2$) (6.41 wt% and 0.88 wt%; see Supplemental Data, Table S1). The mineral may have formed by the reaction of kaolinite and quartz in aluminous, Fe-poor, clay-rich zones within late diagenetic or anchimetamorphic zones under low-pressure (~2 kbar) and low-temperature (~240°–260°C) conditions (Frey, 1987).

The KYM is dominated by well-bedded, dark-gray limestones that give rise to a mixture of concentric and chevron-style, disharmonic, and polyharmonic, type folds (Fig. 11). Although the frequent bedding enables flexural-slip–type folding to develop, there are sufficient variations in

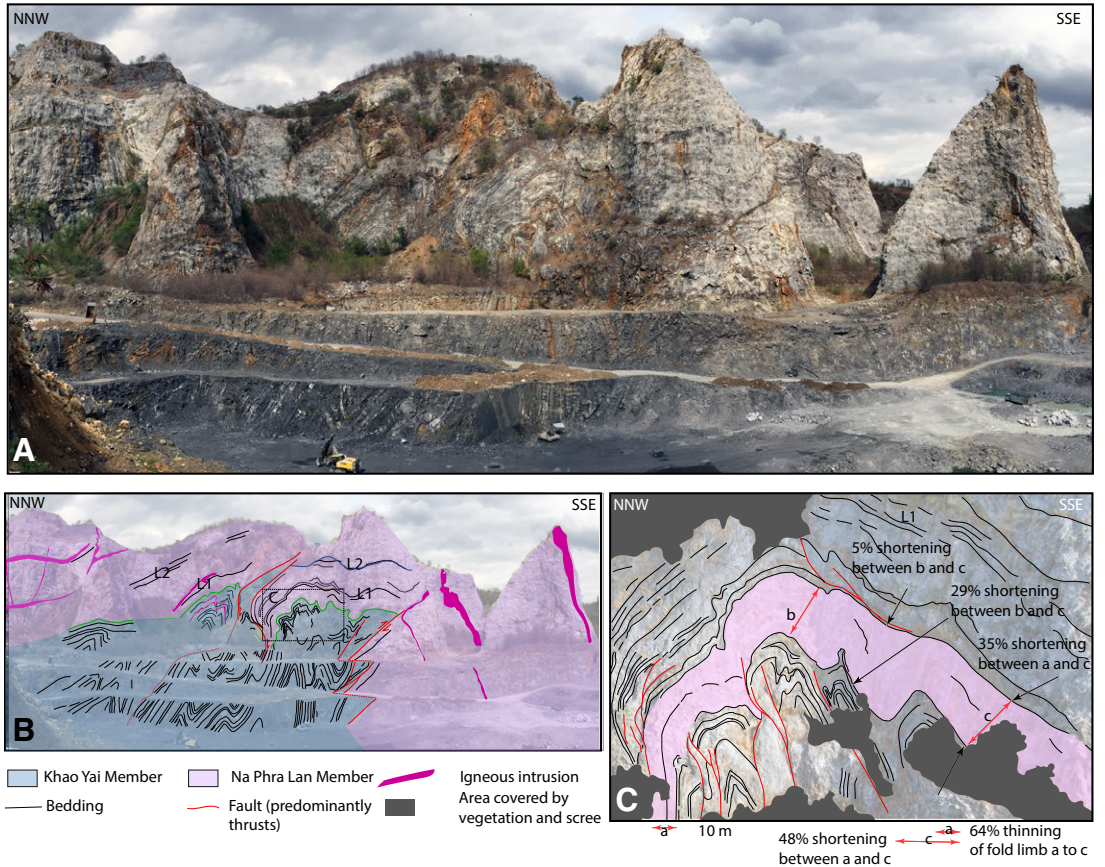

Figure 7. View to the SE of quarry KT4. See Figure 2C for location. (A) Uninterpreted photo; (B) interpreted photo. This is the most extensive quarried outcrop in the area, and displays more weakly deformed Na Phra Lan Member massive carbonates overlying well-bedded tight to isoclinally folded dark-gray to black limestones of the Khao Yai Member. On the SSE side, a south-directed thrust locally emplaces the Khao Yai Member over the Na Phra Lan Member. (C) Interpreted photo of detailed part of KT4 quarry (see Fig. 3C for location). The pink unit lies at the base of the Na Phra Lan Member. The base of the member is strongly folded by secondary folds to the larger anticline. The unit shows considerable thinning (64%) into the forelimb of the large anticline passing from (C) to (A). The lower part of the pink interval shows more line-length shortening at the base (48%) and top (35%), particularly in the interval between arrows (B) and (C) (29% base, 5% top).

bedding thickness and shale content that the fold style is not a simple harmonic one (Fig. 11). Within the same quarry cliff face, thicker-bedded units (3–4 m thick) tend to deform by concentric folding, while adjacent thinner-bedded units form chevron folds, often with similar fold geometry. Such a style creates room problems in the fold hinges, where material from the thinned fold limbs is transported to the fold hinges. Transport can occur by a variety of processes: wedge thrusts, pressure solution along modified bedding and fault surfaces of the limbs, precipitation of calcite in the hinges, and by intracrystalline deformation and flow. Fold tightness ranges from open to isoclinal. The majority of folds tend to display steeply inclined, ~ENE-WSW– to WNW-ESE–oriented axial surfaces and horizontal to gently dipping fold hinges; locally, in high-strain zones, hinges can steeply plunge. There are also examples of gently inclined axial surfaces on tight to isoclinal folds, particularly on folds lying within ~20 m of the base of the Na Phra Lan Member (Fig. 8). Some mesoscale, fault-related fold geometries can be identified (detachment folds, fault-bend folds, and fault-propagation folds; Morley et al., 2013; Warren et al., 2014); commonly, more complex, buckle-fold geometries are also present (Fig. 7).

Although flexural-slip–type deformation can be demonstrated along the folds (e.g., Fig. 9), the later stages of fold deformation have transitioned from flexural-slip– to pressure-solution–dominated flattening. Elsewhere in the KKFTB, in more shale-prone stratigraphic units (e.g., Phu Phe, Pang Asok, and Nong Pong formations), there are good examples of axial planar cleavage. But development of axial planar cleavage is not favored in the carbonate-dominated sections. Instead, pressure solution is focused on MBSs and wedge thrusts (Figs. 10, 11, and 12), particularly where they are on steeply inclined fold limbs. In more highly strained zones, additional pressure-solution seams develop internally along MBSs. The distribution of shortening associated with pressure solution can be

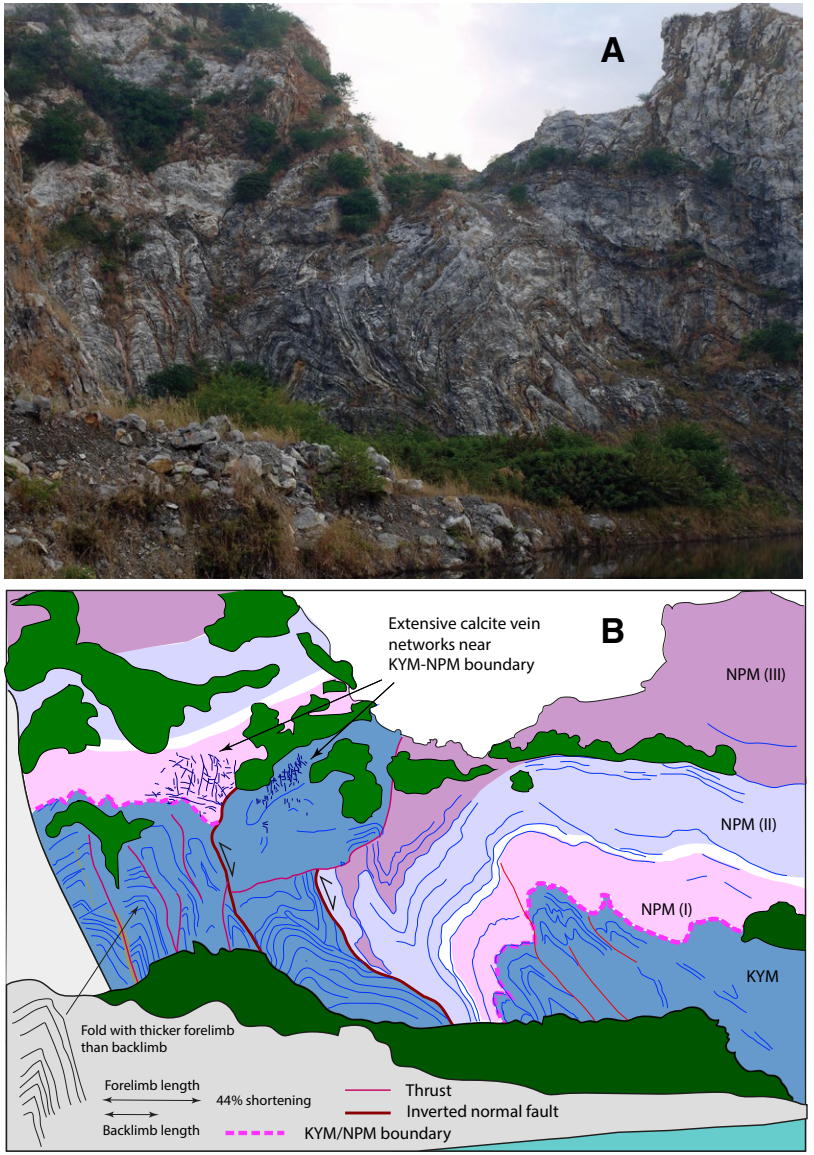

Figure 8. View to the SE of the old quarry part of KT4. This view was taken in 2014, three years prior to the view in Figure 7, when a lake occupied the deeper part of the new quarry that is visible in Figure 7. See Figure 2C for location. (A) Uninterpreted photo, (B) interpreted photo. The base of the Na Phra Lan Member is strongly folded, affected by compression, and verges toward the NNW. It lies deeper than the Na Phra Lan Member on the NNW side of the quarry, and this relationship indicates there was probably inversion of a normal fault.

asymmetric, favoring particular beds, and one fold limb over another (Fig. 12). Hence the distribution of bedding-focused pressure-solution cleavage is significantly different from the more symmetric distribution of axial planar cleavage. The amount of pressure-solution shortening can be large; in Figure 8, the eastern limb of the highlighted fold has shortened by 44% more than the western limb, while in Figure 12 variations in the width of two different intervals show shortening of 57% and 80% (i.e., reduction of interval thickness, primarily by pressure solution). Such high amounts of thinning tend to be confined to the core areas of folds, not across an entire fold. This substantial local elimination of section has resulted in large quantities of calcite vein deposition in adjacent areas of the fold (Fig. 12). These veins range in size from microscopic to hairline (Fig. 10), to large clumps of veins (Fig. 13). Locally, the macroscopic veins can comprise >50% of the rock. Calcite vein arrays can range from simple, readily understood patterns—e.g., veins aligned orthogonal to bedding and all veins striking in a similar direction (±10°), to highly complex arrays (Fig. 10), with masses of veins at the outcrop and microscopic scale that display multiple orientations and crosscutting relationships, together with multiple phases of stylolite growth and recrystallization of older veins. Since the veins in folds are isotopically similar to the host rocks (Warren et al., 2014; Supplemental Data, Fig. S11), they can be inferred to be predominantly the product of pressure solution. The large amount of thinning of section in tight to isoclinal faults appears to be loosely matched by the local abundance of veins in fold cores. Thin sections reveal that at a small scale, extensive pressure-solution seams are present both in the KYM and the NPM, but, generally, the NPM is less intensely deformed by pressure-solution and calcite veins than the KYM. Details of these variations are provided in the Supplemental Data.

As strain increases in folds, a succession of vein and pressure-solution events is developed, leading to closely spaced pressure-solution seams, with older, rotated seams being truncated in places by younger seams, and calcite veins with a wide variety of orientations and geometries (e.g., Figs. 10 and 13; Supplemental Data, Fig. S6). In the highest

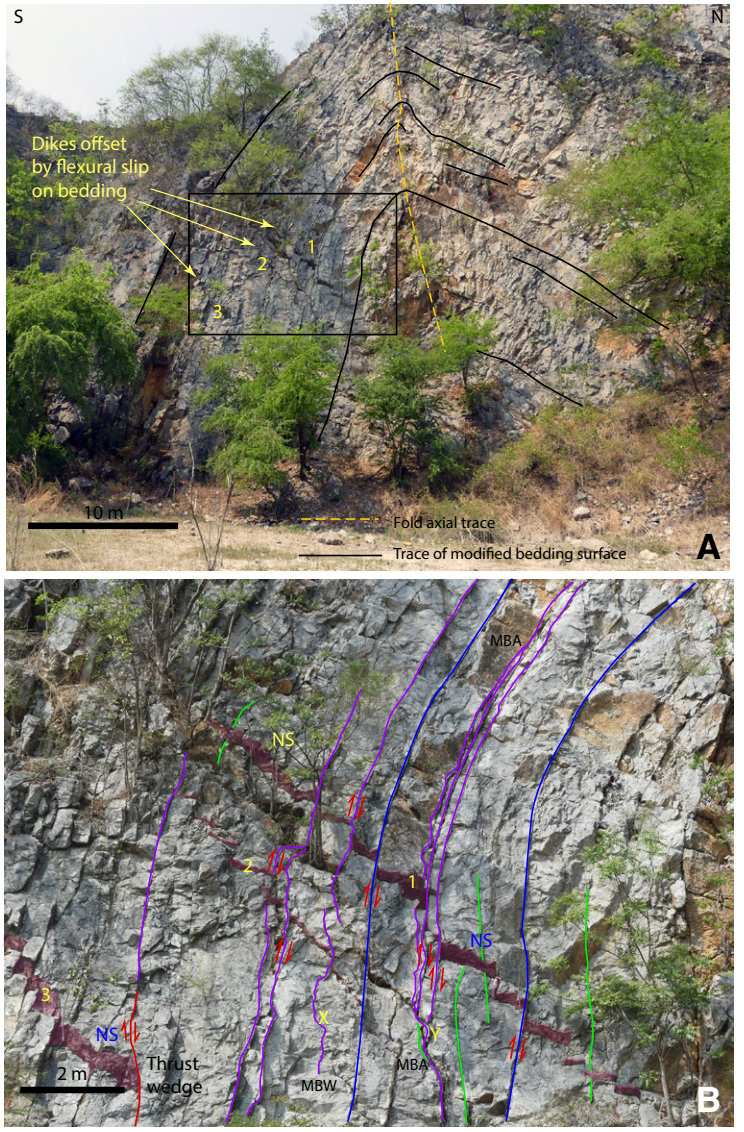

Figure 9. Example of flexural slip folding in a well-bedded limestone of the Khao Khad Formation (see Fig. 2C for location). (A) Overview photo of the outcrop-scale anticline. (B) Detail of photo (A) illustrating pre-kinematic dikes that have been regularly offset by flexural slip motion on bedding during folding. Pressure solution and flexural slip have both played a role in modifying bedding.

strain cores of isoclinal folds, original bedding is largely lost and is replaced by a mixture of contorted veins and dark-colored limestone. Some pressure-solution seams may remain, but instead of the vein-limestone boundaries being sharp fractures, or modified by pressure solution, they tend to become blurred by recrystallization. Locally, where more argillaceous limestones are present, a penetrative cleavage can start to develop (Supplemental Data, Fig. S8). In the cores of isoclinal folds, strain is sufficiently high that local mylonite zones are developed to accommodate flow and flattening of material in the core (Figs. 13B and 13C). These zones display sigma structures in light-colored calcite derived from fossil material and earlier veins and are also overprinted by later veins (Fig. 13), indicating alternation of brittle and ductile processes.

Zones of intense pressure solution, particularly where pressure-solution seams have amalgamated, can produce clay-rich zones that are up to 2–3 cm thick. During late-stage deformation, these clay-rich zones may become slip surfaces, as indicated by the presence of striated, calcite veins that lie in the plane of the seams (Supplemental Data, Fig. S7B). This modification is a late-stage development after the phase when pressure solution starts to disrupt bedding planes that had been undergoing flexural slip.

One further way in which pressure-solution cleavage can develop during fold growth is very different from axial planar cleavage—by causing dissolution of a growing fold crest. There are several examples in, and close to, the study area of anticlines with open to closed limbs; these examples can be seen around the core of an anticline (Supplemental Data, Figs. S12 and S13 [footnote 1]); however, passing upwards, approximately flat-lying modified bedding surfaces are present. At one or more such surfaces, the uplifting anticline

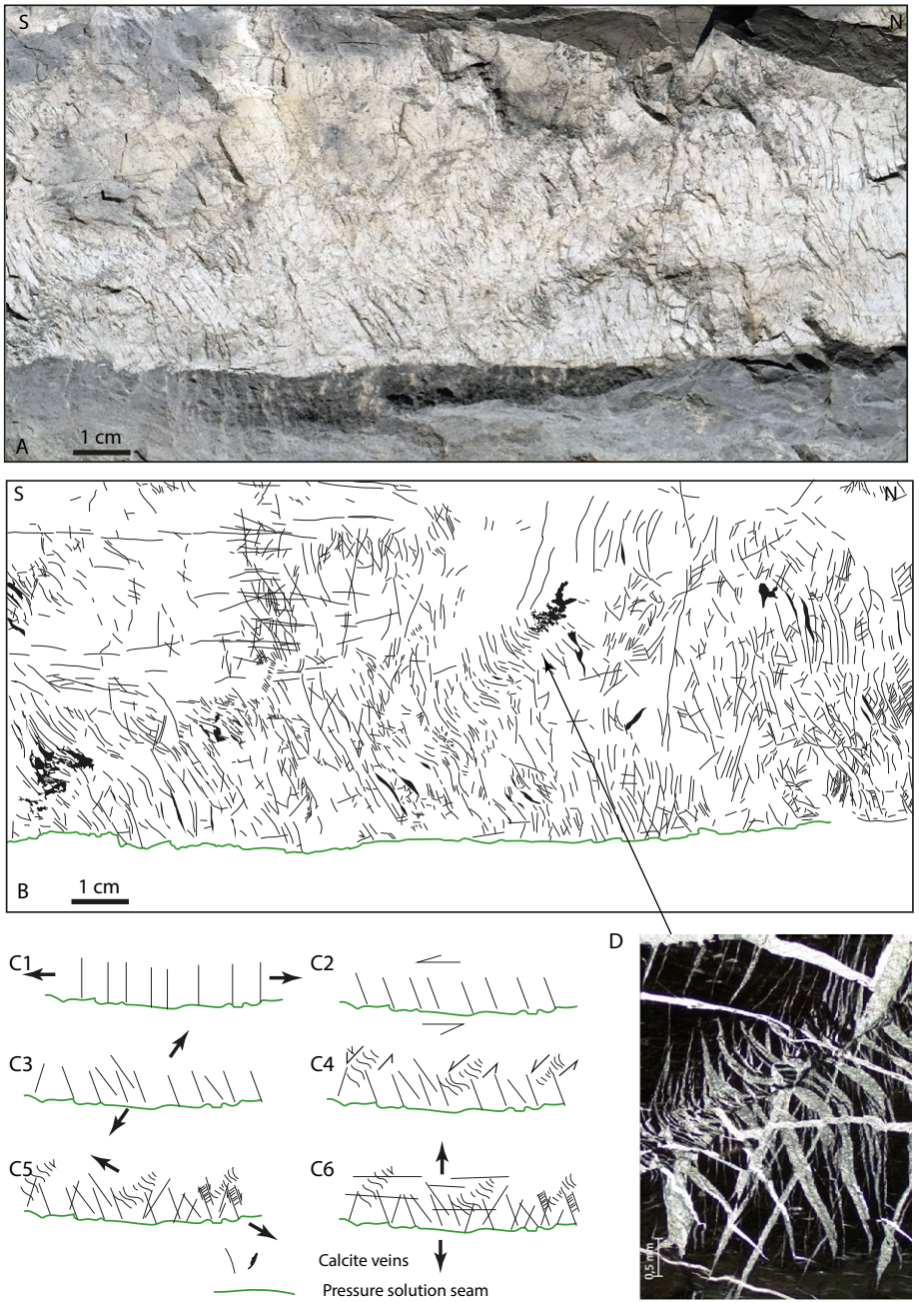

Figure 10. (A) Photograph of numerous narrow calcite-filled fractures affecting a limestone bed in the Khao Yai Member, KT4 quarry. (B) Line drawing of the calcite veins visible in hand specimen. C1–C5 sequence of vein development. The different orientations and styles of the fractures and crosscutting relationships indicate multiple generations of fracture development within a tightly folded sequence. (D) Thin section of part of the sample showing, the white calcite sigmoidal tension gashes in a black micritic limestone. Subhorizontal veins overprint the tension gashes, and the tension gashes overprint diagonal veins inclined from top right to bottom left.

crest has been removed by pressure solution (Supplemental Data, Figs. S12 and S13). This dissolution of vertically growing structures on low-angle surfaces is one way of changing the structural style across a detachment zone. The occurrence of pressure solution that is subparallel to bedding fits with the classic model of tangential longitudinal strain, where flattening strain parallel to bedding (or extensional structures) develop in the outer arc of a parallel fold (e.g., Ramsay, 1967; Shimamoto and Hara, 1976). Figure 7C shows that the internal flattening out of fold amplitude within the basal part of the NPM results in reduction of line-length shortening from 29% to 5% across a 10-m-thick interval. The folds that are reduced in amplitude across the interval are secondary s-type folds on the northern flank of a larger anticline. Across the larger anticline, the basal NPM interval marked by arrows a, b, and c shows considerable thinning (64%) passing from the back limb to the forelimb. Much of this thinning has been accomplished on bed-parallel pressure-solution seams.

Variation in fold style within the KYM occurs in response to the spacing of bedding and position within a fold (Fig. 11). Wedge thrust development is only locally of high intensity in one syncline core, while pressure solution along modified flexural slip bedding surfaces is widespread. Only few original bedding surfaces remain, with most bedding surfaces exhibiting wavy surfaces, modified by pressure solution (Fig. 11). In the areas of more open concentric folds, some bedding surfaces without or only moderately affected by pressure solution are present.

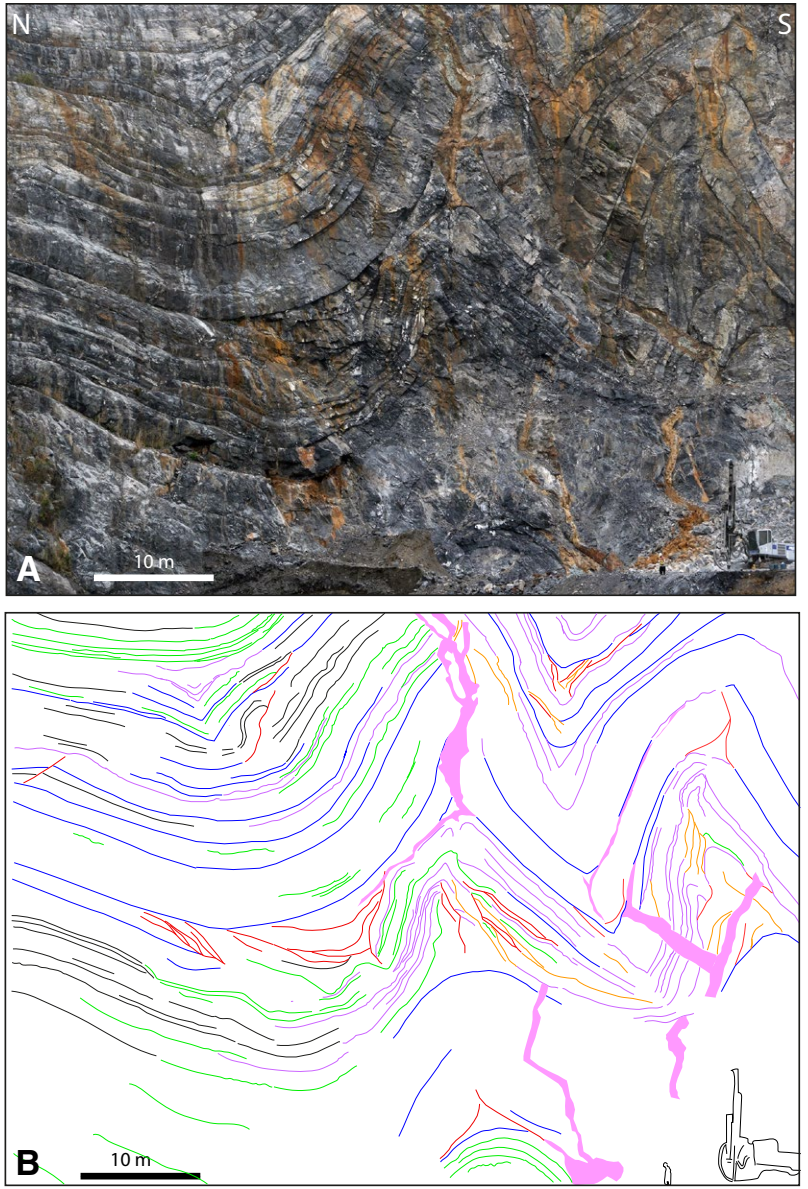

Figure 11. Example of typical folding from the Khao Yai Member (see Fig. 2C for location). (A) Photograph of part of a quarry face showing a range of fold geometries (concentric to similar, rounded to angular, almost chevron style) in different layers, and how bedding thickness and/or spacing influence fold morphology. (B) Line drawing of the folds in A, showing the different types of modification to the bedding surfaces and their spatial variation. See Figure 2B for location.

Stages in the development of folds are schematically illustrated in Figure 14. Initially, flexural slip is shown as dominant during broad to open folding, together with the localized development of thrust wedges. As the fold tightens, flexural slip affects part of the folds, but pressure solution along bedding surfaces becomes important, particularly on more steeply dipping fold limbs. This causes flexural slip to be abandoned in parts of the fold. The mechanical differences between the layers, such as bedding thickness, presence and/or absence of thin shales, and differences in deformation mechanisms present (pressure solution, bedding plane slip, and wedge thrusts) lead to increasing disharmony between the layers as the folds tighten (Fig. 14C). Folds that attained tight to isoclinal geometries and steeply dipping axial planes are strongly affected by flattening by pressure solution and calcite vein formation, which occurs mainly parallel to modified bedding surfaces, and is interpreted to represent an alternative to the formation of axial planar cleavage. This flattening is partly the cause of the broad range of fold geometries (from Class 1 to Class 3: Ramsay, 1967; Fig. 15).

Transition Zone from Khao Yai to Na Phra Lan Member

The change in structural style from the KYM to the NPM varies across the study area and does not necessarily occur at the stratigraphic boundary, despite the sharp change from bedded to massive limestone. In some areas (Figs. 5 and 6), the formation boundary is smooth and approximately marks the top of a change in deformation style, with a transition zone in the upper part of the KYM. In

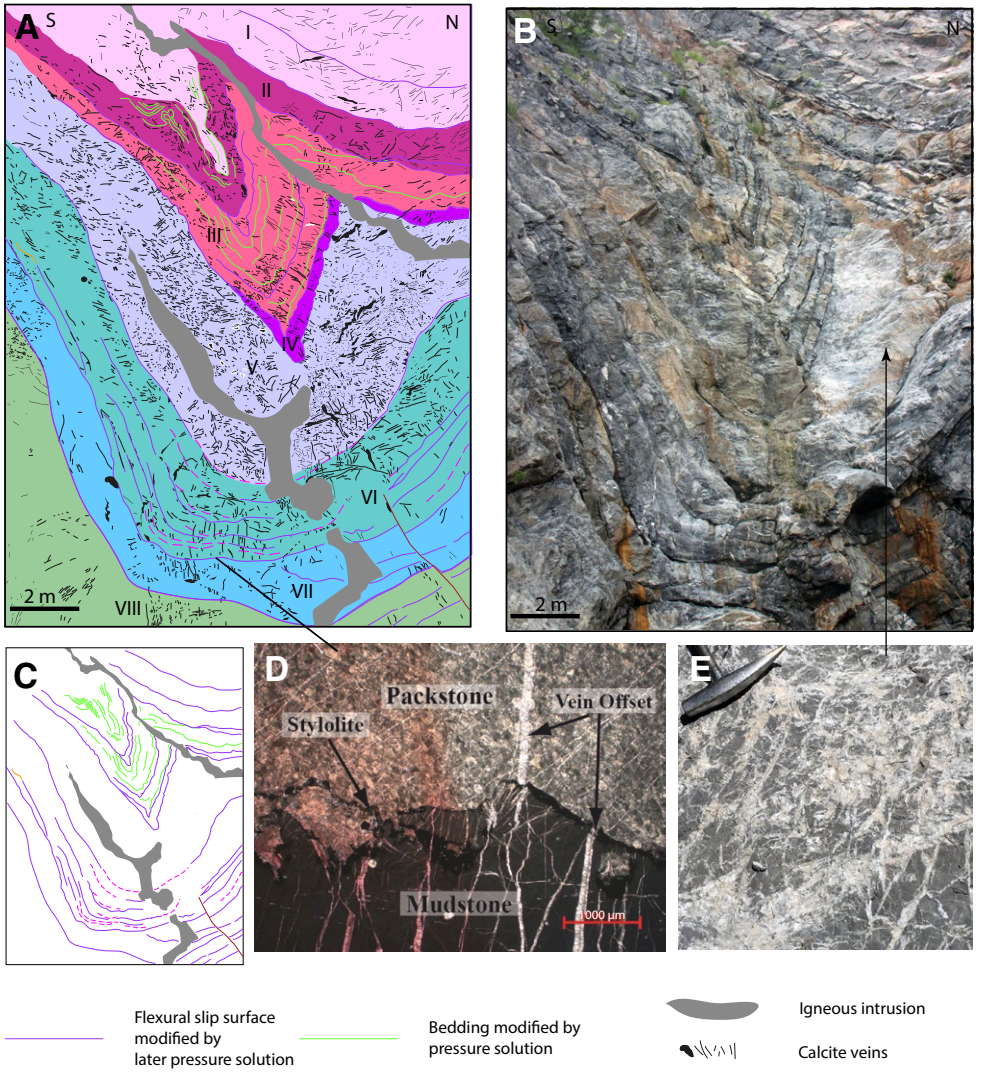

Figure 12. Detailed example of typical folding from the Khao Yai Member (see Fig. 2C for location). (A) Photograph of part of the quarry face focused on a syncline where different layers exhibit considerable different morphologies. Layers III and IV exhibit extreme thinning of the southern fold limb by pressure solution on bedding surfaces. Other layers do not thin so markedly. Layer V contains a very high concentration of calcite veins of various orientations that are probably largely derived from the thinning of layers III and IV. (C) Types of modified bedding shown in B; most bedding surfaces are flexural slip type that have been later modified by pressure solution. (D) Thin section showing pressure solution at interface between a carbonate mudstone and a packstone. Pressure solution on the bedding surface has been syn-tectonic because some tectonic veins are offset at the surface, while others cross-cut it. (E) Example of intense calcite veining near the core of the fold, where >50% of the rock is vein fill.

some areas, one or more thrusts subparallel to, and a few meters below, the KYM-NPM boundary help separate the underlying folded section from the massive limestone (Supplemental Data, Fig. S2). In other examples, there is a transition from steeply dipping fold limbs to gentler dips passing upwards (Fig. 5 and Fig. S3); this transition results in the upper few meters of the KYM lying subparallel to the formation boundary. In one example, the KYM-NPM boundary is folded along with the upper part of the KYM, but folds then die out within approximately the lower 10 m of the NPM (Fig. 7C). In the Saraburi area, a number of examples, of different size anticlines in limestones, die out upwards, with the vertical relief caused by folding being removed by bedding-subparallel pressure solution (Fig. 7C; Figs. S12 and S13). This mechanism within the lower part of the NPM and upper few meters of the KYM helped to limit the vertical extent of folds formed within the KYM.

The strike view of the detachment zone in Figure 4 shows fourfold crests in a distance of 100 m in the hangingwall of a thrust. The tight to isoclinal folds with gently dipping axial surfaces in Figure 5 probably represent the dip-section geometry of these folds. The abrupt lateral closure style of the folds in Figure 4 resembles folds developed during layer-normal shearing described by Alsop et al. (2020), where complex fold patterns arising from differential flow within mass transport complexes create local regions where layer-normal, shearing-related folding is developed in areas trapped between different layer-parallel shear regimes. The strike geometries are reminiscent of sheath folds, but the eye structures are incomplete due to downwards or upwards termination at thrusts or detachments.

The KYM-NPM boundary at quarry KT2 (Fig. 5) comprises a zone of vein material, 4–10 cm thick, with striations lying in the plane of bedding, (353°11°N, on bedding that dips 12° toward 345°N; Figs. 16C, 16D, and 16G). The zone of veining is considerably thicker than the typical flexural slip calcite zones that are <1 cm thick and represents the upper part of the detachment zone. In thin section (Figs. 17D and 17E), the fabric comprises intense bedding-parallel veining, also known as "beef" (see Cobbold et al., 2013, for a global compilation and review).

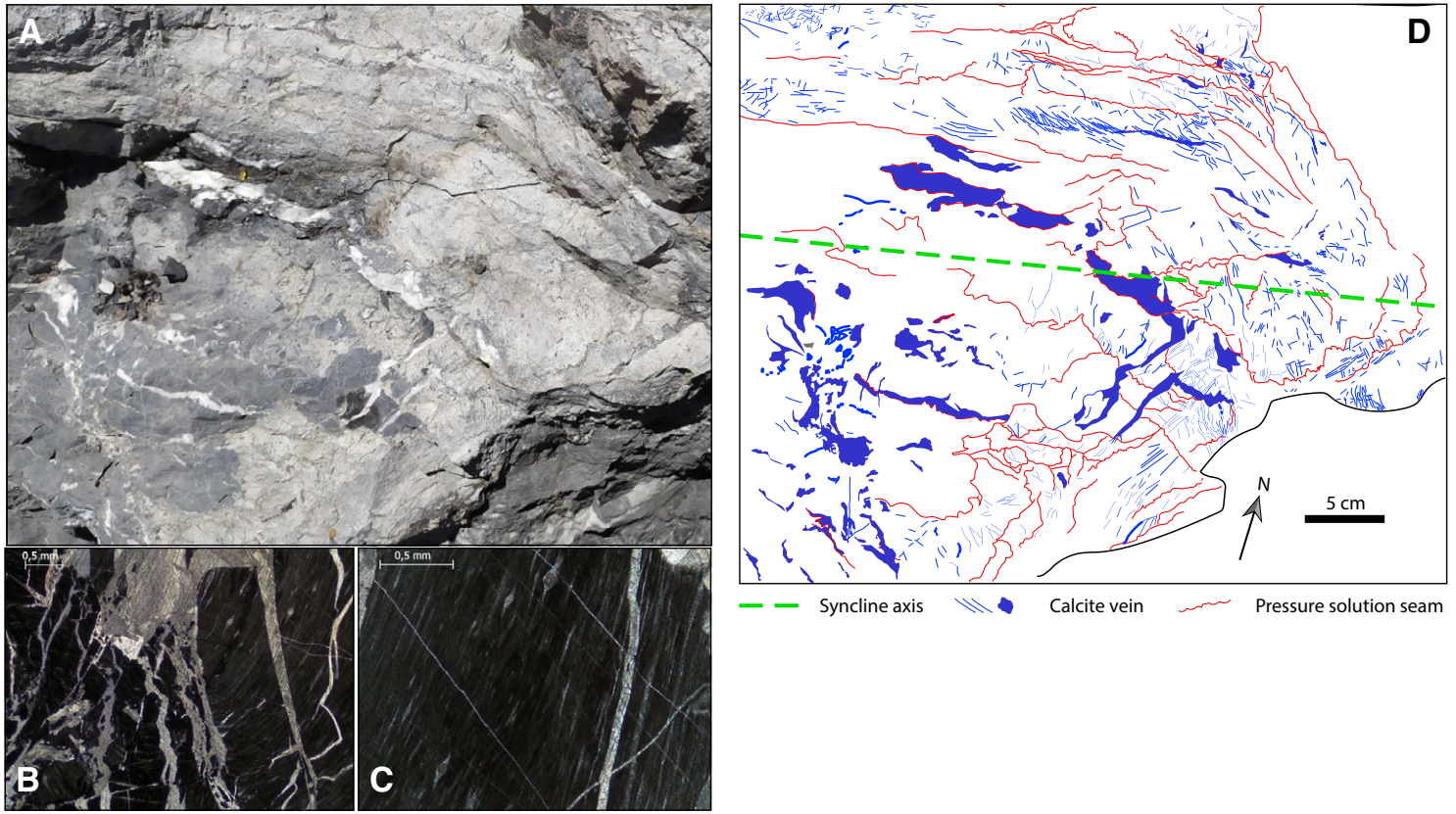

Figure 13. (A) Photograph of the core of a syncline in an isoclinal fold from the Khao Yai Member, quarry KT4 (see Fig. 2C for location of quarry). A dark, almost black limestone, and a dark-gray limestone are present. B and C show the black limestone affected by a ductile shear zone, where old vein and bioclastic material has been stretched and boudinaged. Abundant sigma clasts show a sinistral sense of movement. In areas of lesser strain, sets of thin (few µm thick) veins almost perpendicular to main foliation occur, ranging from undeformed to stretched and folded. The shear zone has been folded before it was fractured. (D) Line drawing of A illustrating the distribution of macroscopic pressure-solution seams (closely spaced, some orientations departing from bedding parallel), and narrow (hairline) and larger calcite veins. The local ductile shear zone reflects intense deformation during the later stages of folding, in the fold core.

The bedding-parallel veins form bundles of few-µm-thick veins that follow the grain boundaries of the host rock, suggesting these are multi-layered veins following the nomenclature of Lee and Wiltschko (2000). This suggests repetitive fracturing and sealing of a dynamically over-pressured system. The original vein calcite of the thin bedding-parallel veins in many places is recrystallized to poikilotopic spar crystals that have incorporated multiple individual veinlets and destroyed older textural relationships. Calcite spar reaches sizes of several mm (Fig. 17E).

In addition to the thin bedding-parallel vein bundles, cm-sized bedding-parallel veins are present, separated from the vein bundles by pressure-solution seams (Figs. 16G and 17E). All calcite crystals, including the poikilotopic spar, show intense twinning, some of which are curved. Pressure-solution surfaces are abundant and are younger than the bedding-parallel veins. Pressure solution occurs both parallel as well as perpendicular to bedding. All bedding-parallel veins as well as pressure-solution seams are crosscut by thin vein sets with three main orientations—subparallel to bedding, perpendicular to bedding, and a conjugate set dipping at ~60° to bedding. Crosscutting relationships between these veins are not systematic, indicating all different generations formed in a continuum.

The 1–2-m-thick section of the KYM underlying the thick veined zone described above is extensively veined, and affected by pressure solution, and has lost the modified bedding planes typically found in the formation. However, in thin section, in places, the rock fabric is not highly deformed,

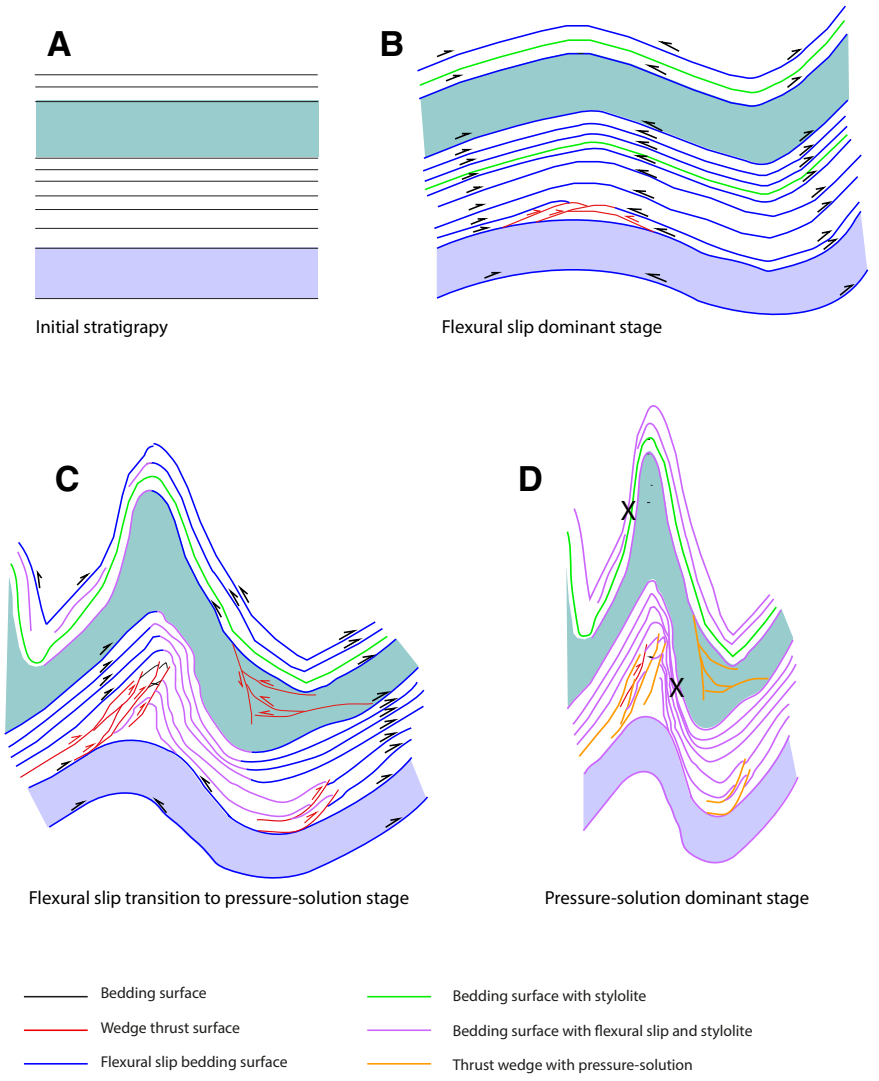

Figure 14. Schematic illustration of fold evolution within the Khao Yai Member (such as the folds in Figs 11 and 12). (A) Initial stratigraphy where different bedding spacing will impact the fold morphology. (B) Early stage folding where flexural slip is dominant, and locally wedge thrusts develop. A few beds do not undergo flexural slip. (C) Tightening of the fault results in more wedge thrust development. On the steeply dipping limb of a fold, pressure solution takes over from flexural slip on the bedding surfaces, but flexural slip continues to operate on other parts of the folds. (D) Final tightening and flattening of the fold, extreme pressure-solution thinning is focused in certain areas of the folds (locations X), flexural slip has ceased, and pressure solution is occurring to greater and lesser degrees on the bedding surfaces.

and fossils, particularly fusulinids, are still present (Fig. 17F). The zones of lesser deformation (Figs. 17B and 17F) alternate with strongly foliated and folded carbonates (Figs. 17C and 17G).

The thick-veined zone (Fig. 17A) is also different from major thrust zones (>1000 m heave) in carbonates in the area, where evidence for shearing occurs in a broad zone, with numerous closely spaced (1 mm–10 mm) pressure-solution seams that form anastomosing networks between carbonate lenses composed of limestone broken up by extensive veining (e.g., Morley et al., 2017). The detachment zone deformation style shows there was some local decoupling at the KYM-NPM boundary, fluids (probably over-pressured) were concentrated at the boundary, and that there is some differential slip between underlying and overlying layers and foliated limestone development, but without the intensity of the major thrust zones.

Na Phra Lan Member

When viewed from a distance, in old quarries, the lower part of the Na Phra Lan Member is massive, with little indication of bedding. However, upon closer inspection, the occasional bedding surface, or group of two to four bedding surfaces clustered over a few meters are commonly present. These surfaces tend to be discontinuous, wavy, and affected by pressure solution. In some places, they are strongly folded and faulted (Figs. 9–11), but in general they are less deformed than the underlying KYM. In other areas (Figs. 5 and 7–9), bedding is gently dipping, or only very gently folded, while the underlying KYM is strongly folded. Overall, the distribution of bedding dips is significantly different in the KYM (a higher proportion of steeply dipping beds, Fig. 2C, a) than the NPM (greater percentage of low-dip values, Fig. 2C, b). In thin section also, the samples of the NPM, while containing veins and pressure-solution seams, are generally less intensely deformed and veined than samples taken from the KYM from the same quarry (particularly KT4). X-ray fluorescence (XRF) analysis of eight samples (see Supplemental Data) indicates there are very low amounts (<0.06 wt%) of Al_2O_3

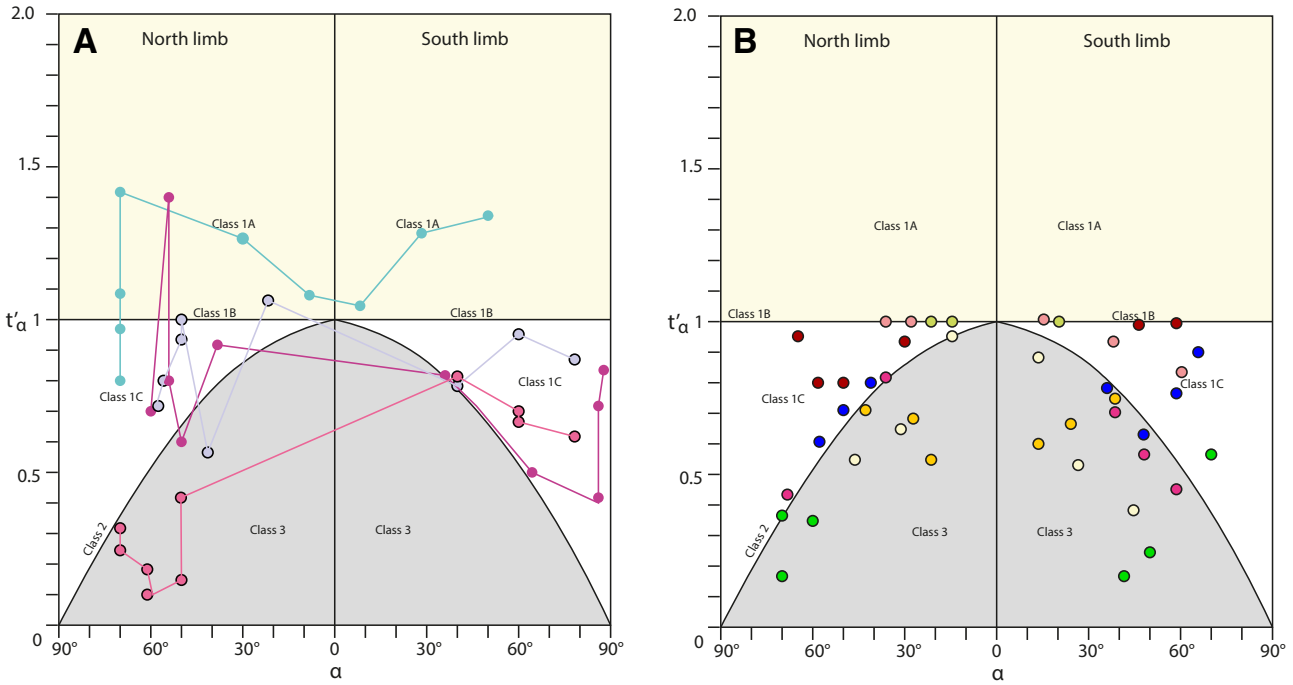

Some intervals plot in class 1 A field

Very few class 1B geometries

The two fold limbs tend to plot in different fields (major asymmetry)

No intervals plot in class 1 A field

Some intervals show class 1B geometries

Both fold limbs tend to plot in similar fields (minor asymmetry)

Figure 15. Plots of variations in fold geometry for different layers within examples of folds in the Khao Yai Member using Ramsay's (1967) t'-α classification. (A) Plot for fold in Figure 12. (B) Plot for folds in Figure 11. Figure 11 shows that some layers have behaved as class 1A folds, while others range between class 1C and class 3. These are related to different layer positions in the fold (class 1C to class 3 are in layers near the fold core, class 1A is farthest from the fold core). In Figure 12, some layers around the more open, concentric folds plot as class 1B. The tighter, chevron-style folds plot in the class 1C to 3 fields. Lines connect points on the same fold.

(reflecting clay mineral content) in the three NPM samples analyzed.

In quarry KT1 (Supplemental Data, Fig. S2 [footnote 1]), the NPM directly above the detachment is exposed. The lowest ~5 m of section above the detachment are composed of highly veined black to dark-gray limestone, which on bedding surfaces shows intense development of multiple conjugate sets of tension gashes (Fig. S15C). In some highly veined areas, remnants of the limestone with strained fossils are present (Figs. S16A and S16B). The section grades upwards into a medium-gray zone of recrystallized limestone ~20 m thick that is remarkable for its low intensity of veins, general absence of fossils, and low intensity of pressure-solution cleavage. In places, early, partially recrystallized pressure-solution seams can be identified (Fig. S15A). Within this limestone, there are locally strongly deformed zones that comprise steeply dipping ENE-WSW– to WNW-ESE–striking calcite veins, and steeply dipping NNW-SSE to NNE-SSW pressure-solution seams a few meters wide (Fig. S15B) and tens of meters long. Possibly these zones represent regions of concentrated fluid flow from the underlying KYM.

The lower NPM in Figure 7 is a medium- to light-gray, micritic to sparry, limestone that is recrystallized in places. Pressure-solution seams are present macroscopically and in thin section, but the NPM lacks the intense, well-developed, closely spaced

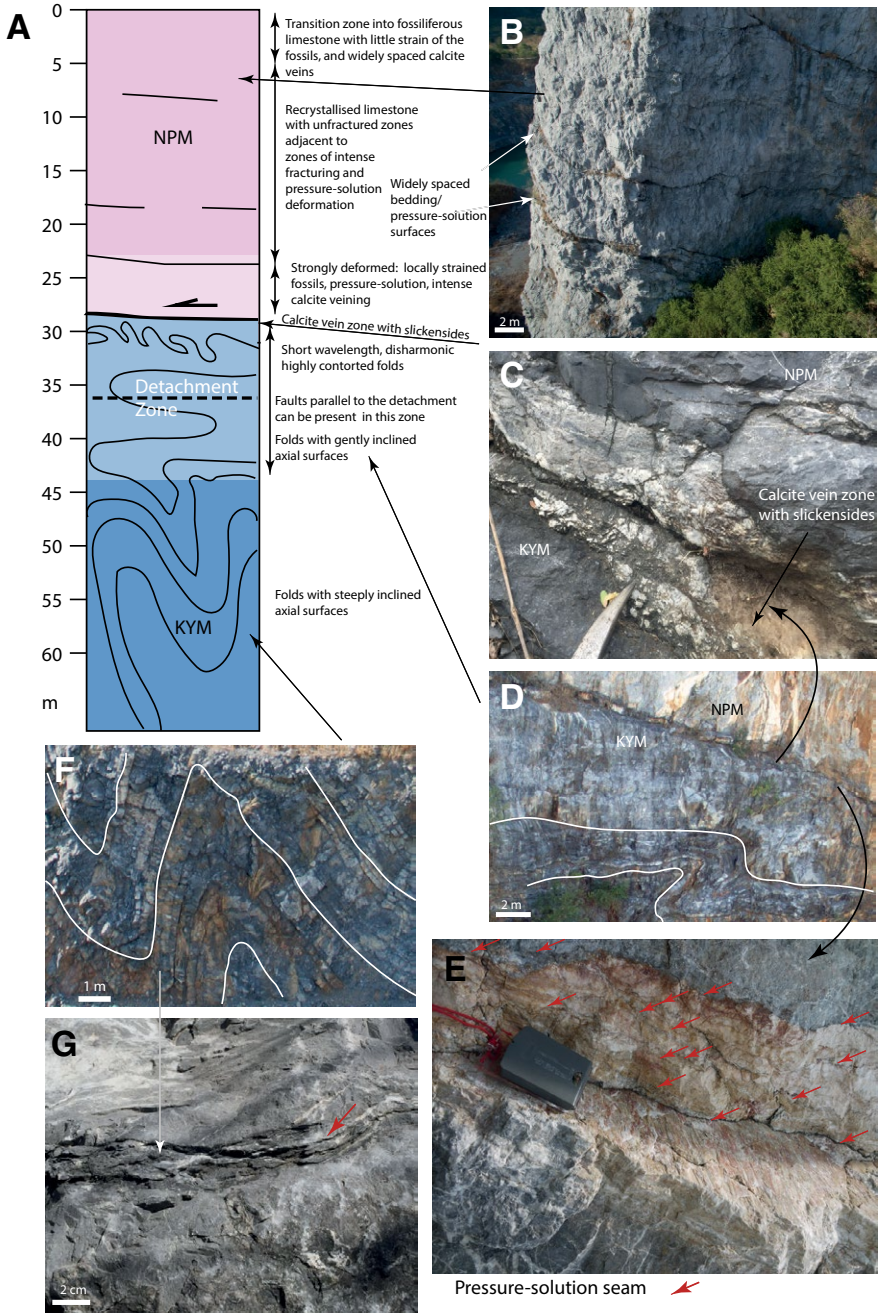

Figure 16. Characteristics of the changes in structural style around the detachment zone between the Na Phra Lan Member (NPM) and the Khao Yai Member (KYM). (A) Schematic section across the transition zone. Pressure-solution and reactivated pressure-solution surfaces as slip horizons (G) play an important role in this folding. In places, short-wavelength disharmonic folding occurs immediately below the detachment zone between the members. This detachment zone is characterized by thick (4–10 cm) calcite veins parallel to bedding, with slickensides (C). Bedding, where present, is weakly folded to unfolded in the NPM. (B) An unusually well-developed sequence of widely spaced bedding surfaces within the NPM, these surfaces are irregular and wavy indicating they are strongly influenced by pressure-solution processes.

pressure-solution cleavage seen in the underlying KYM (Figs. 11–13; Figs. S5, S6, S8, and S9), and also, outside of the detachment zone, lacks the closely spaced calcite micro-veins and hairline veins (Fig. 10). Some macroscopic calcite veins are present in places. Zones of closely spaced veins, 2–4 m wide, traversing quarry faces, are present in places, but these veins, in general, are not as intense, or as well organized as those within the KYM. This vein distribution reflects the lower frequency of bedding surfaces and the consequent absence of flexural slip folds. The best exposed NPM section in Khao Khao is a black "marble" quarry (location KT6, Fig. 2B), which reveals section that stratigraphically lies ~180 m above the base of the NPM. The rock is quarried in cut rectangular blocks such as marble, but is actually a black, fossil-rich micritic limestone. Occasional bedding in the quarry consistently dips north at ~34°. The quarry exposes section in cut blocks with up to 54 m vertical exposure and ~80 m horizontal exposure (Fig. 18). This 100% exposure of slabbed rock shows only occasional, widely spaced, bed-subparallel, pressure-solution cleavage, and undeformed fossils, including corals and bivalves. Mottled sedimentary depositional fabrics are apparent on slabbed surfaces. Calcite veins are present, but are widely spaced, and tend to be orthogonal to bedding (i.e., tilted along with bedding, and dipping ~50°–60° south). Consequently, this large, unique exposure confirms the absence of strong deformation by local folding, pressure solution, and layer-parallel thickening in the NPM compared to the KYM.

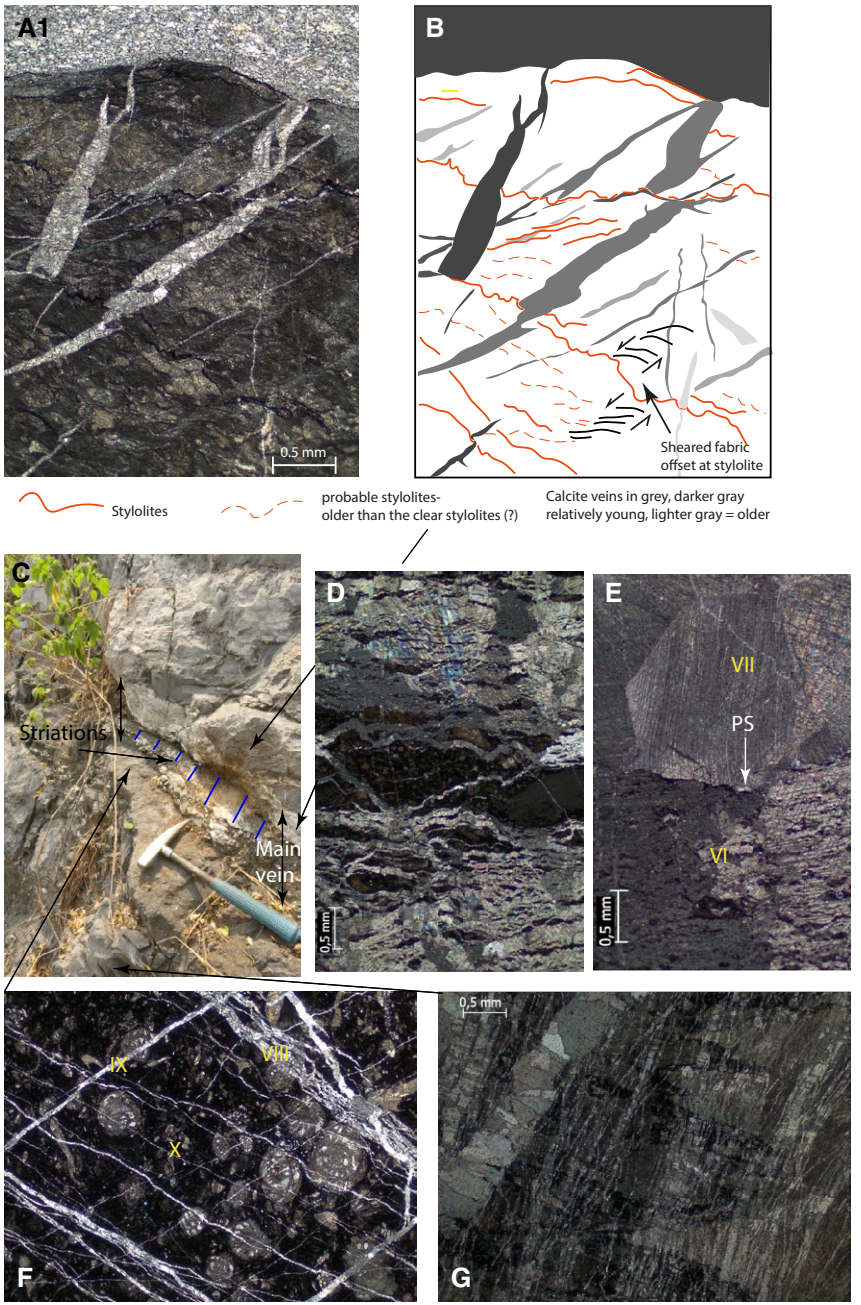

Figure 17. Thin sections showing changes in deformation around a thick, complex calcite vein that marks the upper part of the detachment zone in quarry KT2 (see Fig. 2C for location of quarry. (A) Thin section; (B) sketch of (A), showing multiple phases of calcite veins and stylolites. (C) Outcrop photo (same location as Fig. 16C). (D–E) Thin sections from the main vein. (D) Intense bedding parallel veining with "beef" texture (e.g., Cobbold et al., 2013). The bedding-parallel veins form bundles of few-µm-thick veins that follow the grain boundaries of the host rock, i.e., are multi-layered veins following the nomenclature of Lee and Wiltschko (2000). The texture suggests repetitive fracturing and sealing of a dynamically over-pressured system. (E) Example of poikilotopic recrystallization obscuring the original internal texture of the vein bundles; the boundary between the sparry texture and the vein bundles is a pressure-solution seam. (F) Immediately below detachment is a dark, foraminifera-rich limestone. Bedding parallel veins form bundles few µm thickness (VIII), commonly separated by host lithons (cf. Lee and Wiltschko, 2000; resp. wall-rock inclusion bands, cf. Ramsay, 1980). These vein bundles are crosscut by calcite veins (a few µm to few mm thick) approximately orthogonal to them (IX). A third vein group is oriented ~45° to the other vein groups and crosscuts them. Pressure solution occurs both perpendicular as well as parallel to bedding. (G) Intensely veined dark limestone, 60 cm below the main vein is an intensely veined dark limestone. Folded foliation is crosscut by multiple thin veins (few µm to 0.5 mm thick) that lie perpendicular to the main foliation and fold axial planes.

DISCUSSION

A detachment zone, within a Permian carbonate platform sequence has been identified in the hills around the town of Na Phra Lan. This detachment zone has formed in response to the different deformation characteristics exhibited by dark-gray to black, well-bedded limestones of the Khao Yai Member, and medium- to light-gray (and occasionally dark-gray to black), carbonates of the Na Phra Lan Member. Between these two units lies a transition zone where the structural style changes. While on larger-scale cross sections it is convenient to show the detachment at the boundary of the Khao Yai and Na Phra Lan members, in more detail, the transition zone in some places appears to be mostly within the KYM (Fig. 5), while in other areas, it can continue 10–30 m into NPM (Fig. 7).

Much of the difference in deformation style between the NPM and KYM is related to the

presence or absence of bedding, which in turn is a feature of depositional environment and its subsequent diagenetic history during burial (e.g., Bathurst, 1987). Bedding enabled flexural slip-type folding to dominate initially, and subsequently, bedding facilitated modification of fold shape predominantly by pressure dissolution. Both the presence of bedding and the higher clay content of the KYM carbonates have facilitated different deformation behavior from the NPM. In areas of intense folding within the KYM, a simple comparison of line-length shortening for horizons passing up to the detachment shows that locally, over distances of tens of meters, shortening decreases upwards from 48%–50% to ~10% (Fig. 7C).

Clay particles can greatly enhance deformation by pressure-solution creep and increase strain rates by allowing faster diffusion of solutes between particle contacts and pore spaces (Renard et al., 2001). Clay linings are necessary to cause the localization of dissolution into stylolites, leading to a feedback mechanism where a region with a larger clay fraction will experience enhanced dissolution, accumulate more residual clays, and thus further enhance pressure solution in that region (Aharonov and Katsman, 2009). Numerical models by Aharonov and Katsman (2009) show that a clean rock (i.e., lacking clays) with defects will undergo dissolution at the defect tips, but the amount of dissolution is limited, and the defect undergoes only minor propagation. However, in more argillaceous rock, the presence of clays and their catalyzing effect encourages defect propagation and lengthening, as well as defect thickening leading to stylolite development (Aharonov and Katsman, 2009). These observations regarding clay content are supported by the extensive nature of the pressure-solution deformation in the more argillaceous limestones of the Khao Yai Member and the reduced importance of pressure solution in the cleaner limestones of the Na Phra Lan Member. The presence of bedding-related, pressure-solution cleavage rather than axial planar cleavage is likely to be related to the early-stage concentration of clay parallel to bedding, which resulted in pressure solution continuing to be focused on these zones in the later stages of deformation, rather than creating extensive axial planar cleavage.

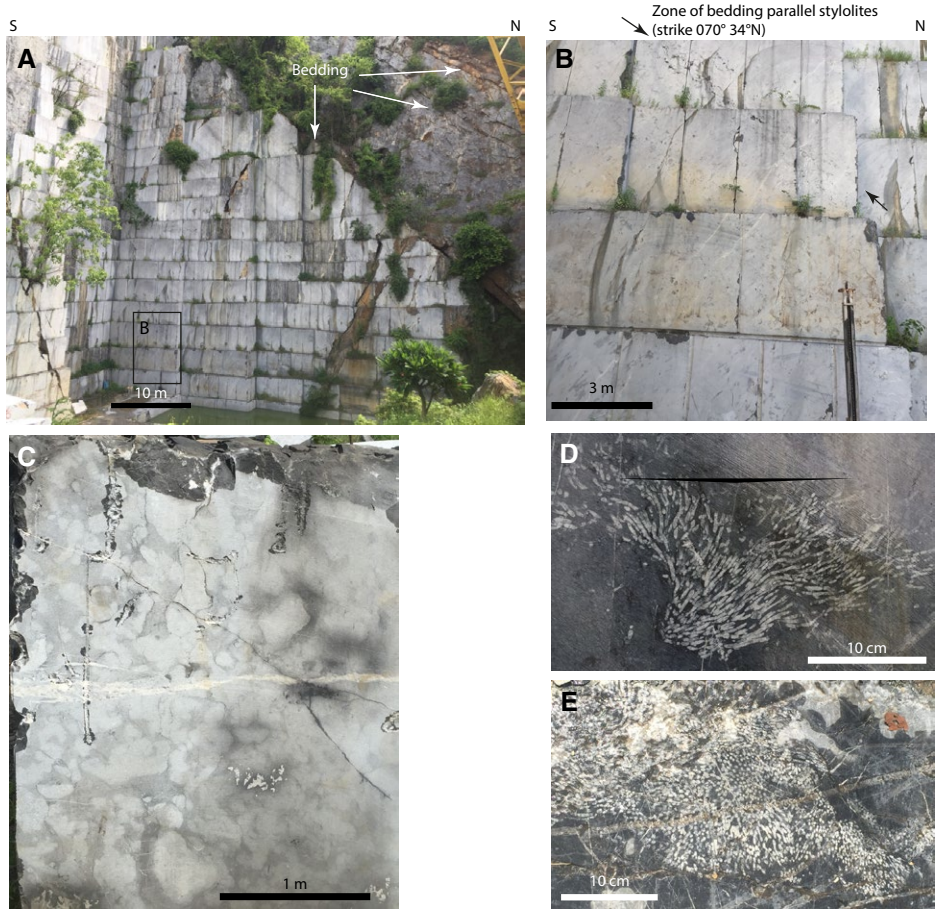

Figure 18. Example of the Na Phra Lan Member, from the black "marble" quarry (KT6, Fig. 2B). (A) Overview of the quarry showing the extensive cutting of rectangular blocks in the quarry. Note the inclined surface at the top of the quarried section is a lithology change to a dark-gray limestone, from the black limestone (weathers to a light color) and follows a bedding surface. (B) Slabbed face demonstrating the scarcity of pressure-solution seams. The zone that is present in this 10-m-thick interval is an early, bedding-parallel narrow zone of multiple stylolites. (C) Black limestone slab, with weathered face showing the highly mottled (by bioturbation?) and undeformed sedimentary structures. Examples of undeformed corals: (D) life position coral in cross section, and (E) Coral exposed on bedding surface.

In many fold and thrust belts, early layer-parallel bulk-shortening strain (LPS) by compaction and/or cleavage formation, occurs prior to the main folding and thrusting stage and can be responsible for shortening up to ~20%–30% (e.g., Gray, 1981; Mitra and Yonkee 1985; Morley, 1986; Protzman and Mitra, 1990; Cochrane et al., 1994; Mitra, 1994; Moore et al., 1995; Butler and Paton, 2010; King et al., 2010; Morley and Naghadeh, 2016; Davis, 2019). Tectonic pressure-solution cleavage can be found as widespread sub-orthogonal-to-bedding orientations indicative of early-stage deformation before significant folding

(Gray, 1981; Marshak and Engelder, 1985; Mitra and Yonkee, 1985; Morley, 1986; Mitra, 1994; Boyer and Mitra, 2019; Davis, 2019), bedding-oblique cleavage developed during folding and thrusting (e.g., Marshak and Engelder, 1985; Morley, 1986), and late-stage flattening including axial planar cleavage (e.g., Ramsay, 1962, 1967; Dewey and McManus, 1964; Hudleston and Stephansson, 1973; Gray, 1981; see reviews in Hudleston and Treagus, 2010, and Gratier et al., 2013). Pressure solution can also be an important process along fault zones, particularly as a deformation mechanism during aseismic creep (Gratier et al., 2013). But in the KKFTB, early-stage tectonic pressure-solution cleavage at a high angle to bedding is rarely seen, and it is the later-stage, pressure-solution modification of bedding that is dominant. Why the carbonates of the KKFTB have departed from the more typical early-stage development of tectonic pressure-solution cleavage is uncertain but may be related to the overall deformation style. In a number of studies, the development of tectonic cleavage is shown to be associated with early-stage shortening above a basal detachment (e.g., Marshak and Engelder, 1985; Boyer and Mitra, 2019). The absence of this type of cleavage in the study area may indicate no simple basal detachment was present. Possibly the Permian rift setting of the Saraburi Group (e.g., Vattanasak et al., 2020) inhibited development of a through-going, early detachment by offsetting any weak layers present by faulting and/or because of stratigraphically discontinuous weak layers. The resulting disrupted pre-thrusting stratigraphy would have favored development of a thick-skinned deformation style, including inversion of normal faults (see discussion in Morley, 2018) and the absence of early tectonic pressure-solution cleavage.

Intra-thrust sheet decoupling of layers in weak rocks such as shale and evaporites gives rise to the classic detachments described in the literature (see reviews in Morley et al., 2011, 2017, 2018, and Ghanadian et al., 2017), where a weak, more ductile material, is an intrinsic part of the detachment (Figs. 1A–1C). The detachment described here differs from such examples because the carbonates are juxtaposed at the detachment zone, and the differences in deformation style are largely related to bedding spacing, which in turn is related to limestone clay content and how effectively pressure solution versus other deformation mechanisms have developed.

The observations of deformation style within the NPM lead to the question: if thrusts in the NPM are relatively infrequent, folds are generally absent to only gentle to open, pressure-solution cleavage is present, but lacks the intensity seen in more argillaceous limestones, and fossils show little strain, how did the NPM shorten as much as the KYM? Although layer-parallel thickening seems an attractive alternative deformation mechanism in areas such as the white marble quarry and the lower ~25 m of the NPM, the presence, in numerous localities, of fossils that are not strongly strained (Fig. 18, for example) indicates that layer-parallel thickening is not the solution for the bulk of the NPM section. The NPM is too strongly eroded and discontinuous for large-scale structures to be identified and measured for shortening, in order to demonstrate that the large-scale structures are the solution to the discrepancy in observed local shortening between the NPM and KYM. However, large-scale structures appear to be the only viable solution (Fig. 19). In the Khao Khao area, there are two large thrusts (Figs. 6 and 7) that cut across the NPM and KYM that could, for example, have increased in displacement upwards within the NPM in order to help balance the extra shortening

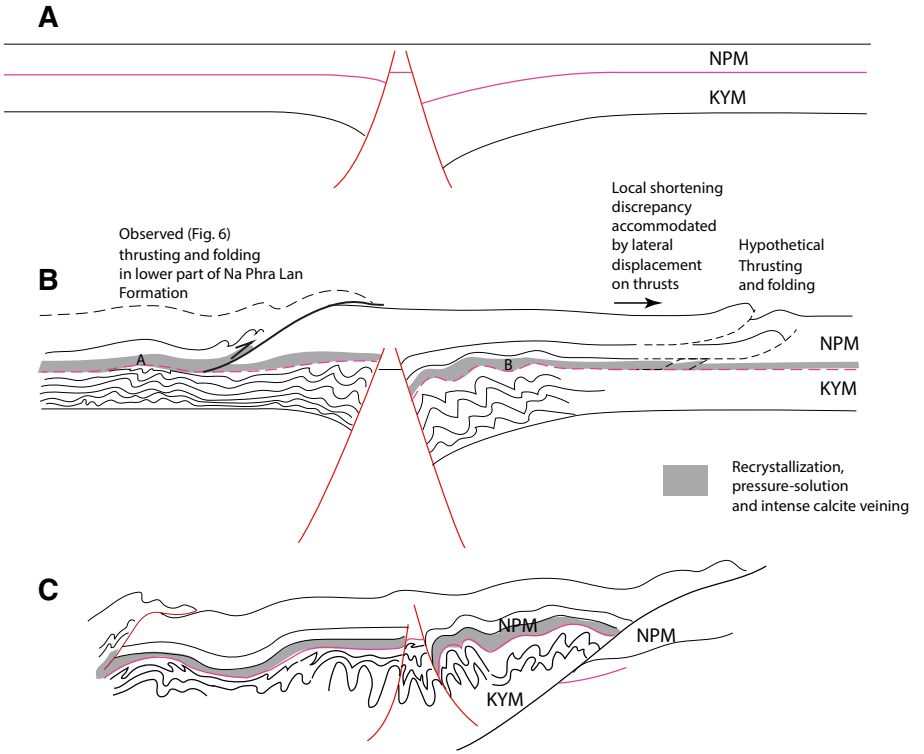

Figure 19. Schematic cross section illustrating the differences in deformation style between the Na Phra Lan Member (NPM) and the Khao Yai Member (KYM). (A) Initial geometry, with the presence of some older extensional faults. (B) Shortening of the members, including inversion of the normal faults. Shorter-wavelength structures are developed in the KYM than in the NPM. (C) Final deformation stage after folds have further tightened and thrusting has occurred.

observed in the KYM (Fig. 19). Unfortunately, the absence of distinctive stratigraphic markers and extensive erosion of the NPM mean that thrust offset within the NPM cannot be determined.

There are few studies in the literature that describe late flattening by pressure solution that departs from classic axial planar cleavage, but one is that of the Pindos Fold-Thrust Belt (Davis, 2014, 2019), where flexural folds are developed in pseudo-bedding. However, significant differences within the study area are the presence of early tectonic pressure-solution cleavage in the Pindos example (at a high angle to bedding) and the intensity of the pressure-solution–related pseudo-bedding. Ramsay's (1967) t'-α classification shows the considerable variety of fold shapes and departures from simple fold morphologies caused predominantly by the effects of mechanical stratigraphy and late flattening (see, for example, Ramsay, 1967; Hudleston and Stephansson, 1973; Hudleston and Treagus, 2010; Davis, 2019). The folds in this study show very similar variations. Simpler, more open folds tend to either follow the Class 1B line or fall in the Class 1C field (i.e., parallel to similar folds), while as the folds tighten up, or thinner beds depart from the deformation style of thicker beds, they fall into the Class 2 and 3 fields (Fig. 15). In folds more affected by the late-stage flattening associated with pressure-solution cleavage, the geometry of a single layer can become much more variable, and in the more extreme cases, may range across all five classes (Fig. 15).

CONCLUSIONS

Classic detachments are generally defined by a weak lithology, often accompanied by high overpressures. The detachment in this study describes a more unusual case of a detachment that occurs within a relatively strong carbonate lithology, whose main variations are bedding spacing and clay content.

The detachment within the carbonate sequence around the town of Na Phra Lan is developed as a consequence of the transition from dark-gray to black, well-bedded, clay-rich limestones of the KYM, to much less frequently bedded, medium- to light-gray, commonly recrystallized limestones and marbles of the NPM. The KYM display much tighter to even isoclinal, shorter-wavelength folds than the NPM. In more detail, the folding began as flexural slip-type folding, in places displaying classic Z-M-S–type secondary folding, and later underwent flattening by pressure solution along early bedding surfaces and between and subparallel to the bedding.

Pressure solution appears to have played a dominant role throughout the structural development, first forming early diagenetic bedding; this bedding then influenced fold style, and later tectonic pressure solution preferentially followed the older pressure-solution features rather than form axial planar cleavage. Throughout this history, the initial concentrations of clays within the limestones dictated how the diagenetic bedding would develop, and later the bed-parallel concentrations of clay minerals both influenced development of bed-parallel dissolution over axial planar cleavage and the formation of local shear surfaces (particularly those accommodating flexural slip) and the differences in deformation style between the KYM and the NPM.

The detachment zone is transitional over tens of meters and varies from locality to locality. In some places, the change in deformation style occurs at the boundary between the members; in other places, it occurs gradationally tens of meters into the NPM. The change in deformation style involves the loss of tight to isoclinal folds, with steeply dipping to vertical axial planes in the main part of the KYM, by either replacement by folds with low-angle axial planes, thrusts and thrust wedging, bed-parallel shearing, and by pressure solution along bedding-parallel seams (that reduce fold amplitude). Where large folds in the KYM are asymmetric, the gently dipping back limbs can display secondary folds that die out entirely within the upper KYM; whereas, in the forelimb, secondary fold amplitude may diminish vertically but still cross the KYM-NPM formation boundary (Fig. 7C).

At the scale of large outcrops (i.e., 100–300 m long), visible shortening via folding and thrusting is greatest in the KYM and is probably up to 50% (there is extra shortening by pressure solution to be added to this estimate) and can decrease to <10% shortening at the KYM-NPM boundary or within the lower part of the NPM. This variation in shortening implies that deformation within the NPM is being accommodated differently from the KYM, probably by a combination of the following: (1) shortening on longer wavelength and/or spacing folds and thrusts (major contribution); and (2) recrystallization and layer-parallel thickening (minor contribution).

At the temperature of deformation (160 °C–220 °C) undergone by the study area during the Triassic, pressure solution, recrystallization, and even, locally, ductile deformation (e.g., mylonites) could be important deformation mechanisms, but of varying importance in response to the clay content of the carbonates. Pressure-solution shortening was dominant in the KYM, with crystal plasticity being secondary, while in the NPM, pressure solution is present but less dominant and decreases in tectonic significance passing away from the detachment zone. It is inferred that deformation by widely spaced folds and thrusts in the NPM can account for most of the observed differences in local strain between the KYM and NPM (Fig. 19).

ACKNOWLEDGMENTS

We would like to thank the quarry owners of the Na Phra Lan area for permitting access to their quarries and PTTEP, Chiang Mai University, and the Petroleum Geoscience Program at Chulalongkorn University for helping with fieldwork in the area over many years. We thank colleagues Nares Sattayarak, Punya Charusiri, Thasinee Charoentitirat, Rosalind King, Alan Collins, Francesco Arboit, Rowan Hansberry, Sopon Pongwapee, and Hathai Vattanasak for discussions and help with investigating the geology of the area over the years. We would also like to thank two anonymous reviewers for very useful and constructive reviews that considerably helped to improve the manuscript.

REFERENCES CITED

Aharonov, E., and Katsman, R., 2009, Interaction between pressure solution and clays in stylolite development: Insights from modelling: American Journal of Science, v. 309, p. 607–632, https://doi.org/10.2475/07.2009.04.

Alsop, G.I., Weinberger, R., Marco, S., and Levi, T., 2020, Distinguishing coeval patterns of contraction and collapse around flow lobes in mass transport deposits: Journal of Structural Geology, v. 134, 104013, https://doi.org/10.1016/j.jsg.2020.104013.

Altermann, W., Grammel, S., Ingavat, R., Nakornsri, N., and Helmcke, D., 1983, On the evolution of the Palaeozoic terrains bordering the Northwestern Khorat Plateau: Conference on the Geology and Mineral Resources of Thailand, Department of Mineral Resources, Bangkok, November, 5 p.

Arboit, F., Collins, A.S., King, R., Morley, C.K., and Hansberry, R., 2014, Structure of the Sibumasu-Indochina collision, central Thailand: A section through the Khao Khwang Fold and thrust belt: Journal of Asian Earth Sciences, v. 95, p. 182–191, https://doi.org/10.1016/j.jseaes.2014.06.016.

Arboit, F., Collins, A.S., Morley, C.K., King, R., and Amrouch, K., 2016a, Detrital zircon analysis of the southwest Indochina terrane, central Thailand: Unravelling the Indosinian orogeny: Geological Society of America Bulletin, v. 128, p. 1024–1043, https://doi.org/10.1130/B31411.1.

Arboit, F., Collins, A.S., Morley, C.K., Jourdan, F., King, R., Foden, J., and Amrouch, K., 2016b, Geochronological and geochemical studies of mafic and intermediate dikes from the Khao Khwang Fold and Thrust Belt: Implications for petrogenesis and tectonic evolution: Gondwana Research, v. 36, p. 124–141, https://doi.org/10.1016/j.gr.2016.04.005.

Arboit, F., Amrouch, K., Morley, C., Collins, A.S., and King, R., 2017, Palaeostress magnitudes in the Khao Khwang fold-thrust belt, new insights into the tectonic evolution of the Indosinian orogeny in central Thailand: Tectonophysics, v. 710–711, p. 266–276, https://doi.org/10.1016/j.tecto.2017.01.008.

Barber, A.J., Ridd, M.F., and Crow, M.J., 2011, The origin, movement and assembly of the pre-Tertiary tectonic units of Thailand, *in* Ridd, M.F., Barber, A.J., and Crow, M.J., eds., The Geology of Thailand: Geological Society of London, p. 507–537, https://doi.org/10.1144/GOTH.19.

Bathurst, R.G.C., 1987, Diagenetically enhanced bedding in argillaceous platform limestones: Stratified cementation and selective compaction: Sedimentology, v. 34, p. 749–778, https://doi.org/10.1111/j.1365-3091.1987.tb00801.x.

Booth, J.E., and Sattayarak, N., 2011, Subsurface Carboniferous–Cretaceous geology of Northeast Thailand, *in* Ridd, M.F., Barber, A.J., and Crow, M.J., eds., The Geology of Thailand: Geological Society of London, p. 185–222, https://doi.org/10.1144/GOTH.9.

Boyer, S.E., and Mitra, G., 2019, Fold duplexes: Journal of Structural Geology, v. 125, p. 202–212, https://doi.org/10.1016/j.jsg.2018.07.008.

Bunopas, S., 1981, Palaeogeographic History of Western Thailand and Adjacent parts South-East Asia-A Plate Tectonics Interpretation [Ph.D. thesis]: Victoria University of Wellington.

Burkhard, M., 1993, Calcite twins, their geometry, appearance and significance as stress-strain markers and indicators of tectonic regime: A review: Journal of Structural Geology, v. 15, p. 351–368, https://doi.org/10.1016/0191-8141(93)90132-T.

Butler, R.W., and Paton, D., 2010, Evaluating lateral compaction in deepwater fold and thrust belts: How much are we missing from "nature's sandbox"?: GSA Today, v. 20, no. 3, p. 4–10, https://doi.org/10.1130/GSATG77A.1.

Chantong, C., 2005, Structural Evolution of the Khorat Plateau, Thailand [Ph.D. thesis]: Leeds, England, The University of Leeds, 793 p.

Chonglakmani, C., and Fontaine, H., 1992, The Lam Narai-Phetchabun region: A platform of Early Carboniferous to Late Permian age, *in* Charusiri, P., Jarupongsakul, S., and Pisutha-arnond, V., eds., Proceedings of the Technical Conference on Development Geology for Thailand into the Year 2000: Bangkok, Thailand, p. 39–98.

Chonglakmani, C., 2001, The Saraburi Group of North-Central Thailand: Implication for Geotectonic Evolution: Gondwana Research, v. 4, p. 597–598, https://doi.org/10.1016/S1342-937X(05)70400-7.

Cloos, E., 1964, Wedging, bedding plane slip, and gravity tectonics in the Appalachians: Geological Society of America, Abstracts with Programs, v. 76, p. 239.

Cobbold, P.R., Zanella, A., Ruffet, G., Rodrigues, N., and Loseth, H., 2013, Bedding-parallel fibrous veins (beef and cone-in-cone): Worldwide occurrence and possible significance in terms of fluid overpressure, hydrocarbon generation and mineralization: Marine and Petroleum Geology, v. 43, p. 1–20, https://doi.org/10.1016/j.marpetgeo.2013.01.010.

Cochrane, G.R., Moore, J.C., McClay, M.E., and Moore, G.F., 1994, Velocity and inferred porosity model of the Oregon accretionary prism from multichannel seismic reflection data: Journal of Geophysical Research, v. 99, p. 7033–7044, https://doi.org/10.1029/93JB03206.

Dahlstrom, C.D.A., 1969, The upper detachment in concentric folding: Bulletin of Canadian Petroleum Geology, v. 17, p. 326–346.

Davis, G.H., 2014, Quasi-flexural folding of pseudo-bedding: Geological Society of America Bulletin, v. 126, p. 680–701, https://doi.org/10.1130/B30963.1.

Davis, G.H., 2019, Partitioned tectonic shortening, with emphasis on outcrop-scale folding and flattening, Pindo fold-and-thrust belt, Peloponnese, Greece: Canadian Journal of Earth Sciences, v. 56, p. 1181–1201, https://doi.org/10.1139/cjes-2018-0210.

Davis, D.M., and Engelder, T., 1985, The role of salt in fold-and-thrust belts: Tectonophysics, v. 119, p. 67–88, https://doi.org/10.1016/0040-1951(85)90033-2.

Dawson, O., and Racey, A., 1993, Fusuline-calcareous algal biofacies of the Permian Ratburi Limestone, Saraburi, Central Thailand: Journal of Southeast Asian Earth Sciences, v. 8, p. 49–65, https://doi.org/10.1016/0743-9547(93)90007-C.

Dean, S.L., Morgan, J.K., and Fournier, T., 2013, Geometries of frontal fold and thrust belts: Insights from discrete element simulations: Journal of Structural Geology, v. 53, p. 43–53, https://doi.org/10.1016/j.jsg.2013.05.008.

de Sitter, L.U., 1958, Boudins and parasitic folds in relation to cleavage and folding: Geologie & Mijnbouw, v. 20, p. 277–288.

Dew, R.E.C., King, R., Collins, A.S., Morley, C.K., Arboit, F., and Glorie, S., 2018, Stratigraphy of deformed Permian Carbonate reefs in Saraburi Province, Thailand: Journal of the Geological Society, London, v. 175, p. 163–175.

Dewey, J.F., and McManus, J., 1964, Superposed folding in the Silurian Rocks of Co. Mayo, Eire: Geological Journal, v. 4, no. 1, p. 61–76, https://doi.org/10.1002/gj.3350040106.

Ferrill, D.A., Morris, A.P., Evans, M.A., Burkhard, M., Groshong, R.H., and Onasch, C.M., 2004, Calcite twin morphology: A low-temperature deformation geothermometer: Journal of Structural Geology, v. 26, p. 1521–1529, https://doi.org/10.1016/j.jsg.2003.11.028.

Frey, M., 1987, The reaction-isograd kaolinite + quartz = pyrophyllite + H_2O: Schweizerische Mineralogische und Petrographsiche Mitteilungen, p. 67, p. 1–11.

Geiser, P.A., 1988, The role of kinematics in the construction and analysis of geological cross sections in deformed terranes, *in* Mitra, G., and Wotal, S., eds., Geometries and Mechanisms of Thrusting with special reference to the Appalachians: Geological Society of America Special Paper 222, p. 47–76, https://doi.org/10.1130/SPE222-p47.

Ghanadian, M., Faghih, A., Fard, I.A., Kusky, T., and Kusky, T., 2017, On the role of incompetent strata in the structural evolution of the Zagros Fold-Thrust Belt, Dezful Embayment, Iran: Marine and Petroleum Geology, v. 81, p. 320–333, https://doi.org/10.1016/j.marpetgeo.2017.01.010.

Gratier, J.-P., Dysthe, D., and Renard, F., 2013, The role of pressure solution creep in the ductility of Earth's upper crust, *in* Dmowska, R., ed., Advances in Geophysics: Amsterdam, Elsevier, v. 54, p. 47–179.

Gray, D.R., 1981, Cleavage-fold relationships and their implications for transected folds: an example from southwest USA: Journal of Structural Geology, v. 3, p. 265–277, https://doi.org/10.1016/0191-8141(81)90022-5.

Hansberry, R.L., King, R., Collins, A.S., and Morley, C.K., 2014, Complex structure of an upper-level shale detachment zone: Khao Khwang fold and thrust belt, Central Thailand: Journal of Structural Geology, v. 67, p. 140–153, https://doi.org/10.1016/j.jsg.2014.07.016.

Hansberry, R.L., Collins, A.S., King, R.C., Morley, C.K., Gize, A.P., Warren, J., Lohr, S.C., and Hall, P.A., 2015, Syn-deformation temperature and fossil fluid pathways along an exhumed detachment zone, Khao Khwang fold-thrust belt, Thailand: Tectonophysics, v. 655, p. 73–87, https://doi.org/10.1016/j.tecto.2015.05.012.

Hansberry, R.L., Zwingmann, H., Loehr, S., Collins, A.S., King, R.C., Morley, C.K., and Drysdale, R.N., 2017, Constraining the timing of shale detachment faulting: A geochronological approach: Lithosphere, v. 9, p. 431–440, https://doi.org/10.1130/L612.1.

Hinthong, C., 1981, Geology and Mineral Resources of Changwat Phra Nakhon Si Ayutthaya (ND 47–48), Scale 1:250,000 (in Thai with English summary): Department of Mineral Resources, Geological Survey Report, No. 4, p. 1–105.

Hinthong, C., Chuaviroj, S., Kaewyana, W., Srisukh, S., Oholprasit, C., and Pholachan, S., 1985, Geologic Map of Changwat Pranakhon Si Ayutthaya (sheet ND 47-48, scale 1:250,000): Geological Survey Division, Department of Mineral Resources.

Hudleston, P.J., and Stephansson, O., 1973, Layer shortening and fold shape development in the buckling of single layers: Tectonophysics, v. 17, p. 299–321, https://doi.org/10.1016/0040-1951(73)90044-9.

Hudleston, P.J., and Treagus, S.H., 2010, Information from folds: A review: Journal of Structural Geology, v. 32, p. 2042–2071, https://doi.org/10.1016/j.jsg.2010.08.011.

King, R., Backe, G., Morley, C.K., Hillis, R., and Tingay, M., 2010, Balancing deformation in NW Borneo: Quantifying plate-scale vs gravitational scale tectonics in a delta and deepwater fold-thrust belt system: Marine and Petroleum Geology, v. 27, p. 238–246, https://doi.org/10.1016/j.marpetgeo.2009.07.008.

Kozar, M.G., Crandall, G.F., and Hall, S.E., 1992, Integrated Structural and Stratigraphic Study of the Khorat Basin, Rat Buri Limestone (Permian), Thailand, *in* Piancharoen, C., ed., Proceedings of the National Conference on Geologic Resources

of Thailand: Potential for Future Development, Department of Mineral Resources, Bangkok, Thailand, p. 692–736.

Lee, Y.J., and Wiltschko, D.V., 2000, Fault controlled sequential vein dilation: competition between slip and precipitation rates in the Austin Chalk, Texas: Journal of Structural Geology, v. 22, p. 1247–1260, https://doi.org/10.1016/S0191-8141(00)00045-6.

Letouzey, J., Coletta, B., Vially, R., and Chermette, J.C., 1995, Evolution of salt-related structures in compressional settings, *in* Jackson, M.P.A., Roberts, D.G., and Snelson, S., eds., Salt Tectonics: A Global Perspective: American Association of Petroleum Geologists Memoir, v. 65, p. 41–60.

Marshak, S., and Engelder, T., 1985, Development of cleavage in limestones of a fold-thrust belt in eastern New York: Journal of Structural Geology, v. 7, p. 345–359, https://doi.org/10.1016/0191-8141(85)90040-9.

Meng, Q., and Hodgetts, D., 2019, Structural styles and decoupling in stratigraphic sequences with double decollements during thin-skinned contractional tectonics: Insights from numerical modelling: Journal of Structural Geology, v. 127, https://doi.org/10.1016/j.jsg.2019.103862.

Metcalfe, I., 1999, Gondwana dispersion and Asian accretion: An overview, *in* Metcalfe, I., ed., Gondwana Dispersion and Asian Accretion: Rotterdam, A.A. Balkema, p. 9–28.

Metcalfe, I., 2011, Palaeozoic–Mesozoic history of SE Asia, *in* Hall, R., Cottam, M A., and Wilson, M.E.J., eds., The SE Asian Gateway: History and Tectonics of the Australia-Asia Collision: Geological Society of London Special Publication 355, p. 7–35.

Mitra, G., 1994, Strain variation in thrust sheets across the Sevier fold-and-thrust belt (Idaho-Utah-Wyoming); implications for section restoration and wedge taper evolution: Journal of Structural Geology, v. 16, no. 4, p. 585–602, https://doi.org/10.1016/0191-8141(94)90099-X.

Mitra, G., and Yonkee, W.A., 1985, Relationship of spaced cleavage to folds and thrusts in the Idaho-Utah-Wyoming thrust belt: Journal of Structural Geology, v. 7, p. 361–373, https://doi.org/10.1016/0191-8141(85)90041-0.

Mitra, S., 2002, Fold-accommodation faults: American Association of Petroleum Geologists Bulletin, v. 86, p. 671–693.

Moore, J.C., Moran, K., Mackay, M.E., and Tobin, H., 1995, Frontal thrust, Oregon accretionary prism: geometry, physical properties and fluid pressure, *in* Carson, B., Westbrook, G.K., Musgrave, R.J., and Suess, E., eds., Proceedings of the Ocean Drilling Project, Scientific Results, v. 146 (Pt.1): College Station, Texas, Ocean Drilling Program, p. 359–366.

Morgan, J.K., 2015, Effects of cohesion on the structural and mechanical evolution of fold and thrust belts and contractional wedges: discrete element simulations: Journal of Geophysical Research, Solid Earth, v. 120, p. 3870–3896, https://doi.org/10.1002/2014JB011455.

Morley, C.K., 1986, Vertical strain variations in the Osen-Roa thrust sheet, North-western Oslo Fjord, Norway: Journal of Structural Geology, v. 8, p. 621–632, https://doi.org/10.1016/0191-8141(86)90068-4.

Morley, C.K., 1987, The structural geology of north Hadeland: Norsk Geologisk Tidsskrift, v. 67, p. 39–49.

Morley, C.K., 2018, Understanding Sibumasu in the context of ribbon continents: Gondwana Research, v. 64, p. 184–215, https://doi.org/10.1016/j.gr.2018.07.006.

Morley, C.K., and Naghadeh, D., 2016, Tectonic compaction shortening in the region of isolated listric normal fault, North Taranaki Basin, New Zealand: Basin Research, v. 30, p. 424–436, https://doi.org/10.1111/bre.12227.

Morley, C.K., King, R., Hillis, R., Tingay, M., and Backe, G., 2011, Deepwater fold and thrust belt classification, tectonics, structure and hydrocarbon prospectivity: A review: Earth-Science Reviews, v. 104, p. 37–75, https://doi.org/10.1016/j.earscirev.2010.09.010

Morley, C.K., Ampaiwan, P., Thanudamrong, S., Kuenphan, N., and Warren, J., 2013, Development of the Khao Khwang Fold and Thrust belt: Implications for the geodynamic setting of Thailand and Cambodia during the Indosinian Orogeny: Journal of Asian Earth Sciences, v. 62, p. 705–719, https://doi.org/10.1016/j.jseaes.2012.11.021.

Morley, C.K., von Hagke, C., Hansberry, R.L., Collins, A.S., Kanitpanyacharoen, W., and King, R., 2017, Review of major shale-dominated detachment and thrust characteristics in the diagenetic zone: Part 1, meso- and macro-scopic scale: Earth-Science Reviews, v. 173, p. 168–228, https://doi.org/10.1016/j.earscirev.2017.07.019.

Morley, C.K., von Hagke, C., Hansberry, R., Collins, A., Kanitpanyacharoen, W., and King, R., 2018, Review of major shale-dominated detachment and thrust characteristics in the diagenetic zone: Part II, rock mechanics and microscopic scale: Earth-Science Reviews, v. 176, p. 19–50, https://doi.org/10.1016/j.earscirev.2017.09.015.

Protzman, G.M., and Mitra, G., 1990, Strain fabric associated with the Meade thrust, implications for cross-section balancing: Journal of Structural Geology, v. 12, p. 403–417, https://doi.org/10.1016/0191-8141(90)90030-3.

Ramsay, J.G., 1962, The geometry and mechanism of formation of "similar" type folds: The Journal of Geology, v. 70, p. 309–327, https://doi.org/10.1086/626821.

Ramsay, J.G., 1967, Folding and Fracturing of Rocks: New York, McGraw Hill, 568 p.

Ramsay, J.G., 1974, Development of chevron folds: Geological Society of America Bulletin, v. 85, p. 1741–1754, https://doi.org/10.1130/0016-7606(1974)85<1741:DOCF>2.0.CO;2.

Renard, F., Dysthe, D., Feder, J., Bjorlykke, K., and Jamtveit, B., 2001, Enhanced pressure solution creep rates induced by clay particles: Experimental evidence in salt aggregates: Geophysical Research Letters, v. 28, p. 1295–1298, https://doi.org/10.1029/2000GL012394.

Shimamoto, T., and Hara, I., 1976, Geometry and strain distribution of single-layer folds: Tectonophysics, v. 30, p. 1–34, https://doi.org/10.1016/0040-1951(76)90135-9.

Sone, M., and Metcalfe, I., 2008, Parallel Tethyan sutures in mainland Southeast Asia: New insights for Palaeo-Tethys closure and implications for the Indosinian orogeny: Comptes Rendus Geoscience, v. 340, p. 166–179, https://doi.org/10.1016/j.crte.2007.09.008.

Toriyama, R., 1975, Fusuline fossils from Thailand, Part IX: Permian fusulines from the Rat Buri Limestone in the Khao Phlong Phrah area, Sara Buri, Central Thailand: Memoires of the Faculty of Science: Kyushu University, Series D, v. 23, p. 1–116.

Udchachon, M., Chonglakmani, C., Campbell, H., and Thanee, N., 2007, Late Middle Permian alatoconchid-bearing limestones from the south of the Khao Khwang Platform, central Thailand, *in* Tantiwanit, W., Raksasakulwong, L., Suteetorn, V., et al., eds., Proceedings of The International Conference on Geology of Thailand: Towards Sustainable Development and Sufficiency Economy: Bangkok, Thailand, p. 180–186.

Ueno, K., and Charoentitirat, T., 2011, Carboniferous and Permian, *in* Ridd, M.F., Barber, A.J., and Craw, M.J., eds., The Geology of Thailand: The Geological Society of London, p. 71–136, https://doi.org/10.1144/GOTH.5.

Vattanasak, H., Chonglakamani, C., Feng, Q., and Morley, C.K., 2020, Chert geochemistry, depositional setting, stratigraphic and structural significance for the Permian Nong Pong Formation, Khao Khwang Fold and Thrust Belt, Saraburi, Thailand: Journal of Asian Earth Sciences, v. 191, 104234, https://doi.org/10.1016/j.jseaes.2020.104234.

Wallace, W.K., 1993, Detachment folds and a passive-roof duplex: Examples from the northeastern Brooks Range, Alaska, *in* Solie, D.N., and Tannian, F., eds., Short notes on Alaskan Geology: Alaskan Division of Geological and Geophysical Surveys Professional Report, v. 113, p. 81–99.

Warren, J., Morley, C.K., Charoentitirat, T., Cartwright, I., Ampaiwan, P., Khositchaisri, P., Mirzaloo, M., and Yinguyen, J., 2014, Structural and fluid evolution of Saraburi Group sedimentary carbonates, central Thailand: A tectonically driven fluid system: Marine and Petroleum Geology, v. 55, p. 100–121, https://doi.org/10.1016/j.marpetgeo.2013.12.019.

Wielchowsky, C.C., and Young, J.D., 1985, Regional Facies Variations in Permian rocks of the Phetchabun fold and thrust belt, Thailand, *in* Thanvarachorn, P., Hokjaroen, S., and Youngme, W., eds., Proceedings of the Geology and Mineral Resource Development of Northeastern Thailand: Thailand, Khon Kaen University, p. 41–55.